(19) Europäisches Patentamt
European Patent Office
Office européen des brevets

(11) **EP 2 583 255 B1**

(12) **EUROPEAN PATENT SPECIFICATION**

(45) Date of publication and mention of the grant of the patent:
24.07.2019 Bulletin 2019/30

(21) Application number: **11764280.1**

(22) Date of filing: **16.06.2011**

(51) Int Cl.:
G06T 19/20 *(2011.01)* ***G06T 17/30*** *(2006.01)*
A61B 5/00 *(2006.01)*

(86) International application number:
PCT/IB2011/001683

(87) International publication number:
WO 2012/014036 (02.02.2012 Gazette 2012/05)

(54) METHOD FOR DETERMINING BONE RESECTION ON A DEFORMED BONE SURFACE FROM FEW PARAMETERS

VERFAHREN ZUR BESTIMMUNG EINER KNOCHENRESEKTION AUF EINE DEFORMIERTEN KNOCHENOBERFLÄCHE ANHAND WENIGER PARAMETER

PROCÉDÉ DE DÉTERMINATION D'UNE RÉSECTION OSSEUSE SUR UNE SURFACE OSSEUSE DÉFORMÉE, À PARTIR D'UN NOMBRE LIMITÉ DE PARAMÈTRES

(84) Designated Contracting States:
AL AT BE BG CH CY CZ DE DK EE ES FI FR GB GR HR HU IE IS IT LI LT LU LV MC MK MT NL NO PL PT RO RS SE SI SK SM TR

(30) Priority: **16.06.2010 US 355207 P**

(43) Date of publication of application:
24.04.2013 Bulletin 2013/17

(73) Proprietor: **A² Surgical**
92200 Neuilly-sur-Seine (FR)

(72) Inventors:
- **CHABANAS, Laurence**
  38830 Saint-Pierre-d'Allevard (FR)
- **LAVALLEE, Stéphane**
  38410 Saint-Martin-d'Uriage (FR)
- **TONETTI, Jérôme**
  38000 Grenoble (FR)
- **BYRD, Thomas**
  Nashville, TN 37205 (US)
- **KELLY, Bryan Talmadge**
  Riverside, CT 06878 (US)
- **LARSON, Christopher**
  Edina, MN 55424 (US)

(74) Representative: **Regimbeau**
87 rue de Sèze
69477 Lyon Cedex 06 (FR)

(56) References cited:
US-A1- 2007 249 967

- **FLEUTE M ET AL: "BUILDING A COMPLETE SURFACE MODEL FROM SPARSE DATA USING STATISTICAL SHAPE MODELS: APPLICATION TO COMPUTER ASSISTED KNEE SURGERY", MEDICAL IMAGE COMPUTING AND COMPUTER-ASSISTED INTERVENTION.MICCAI. INTERNATIONAL CONFERENCE. PROCEEDINGS, XX, XX, 1 October 1998 (1998-10-01), pages 879-887, XP000913649,**
- **FLEUTE M ET AL: "INCORPORATING A STATISTICALLY BASED SHAPE MODEL INTO A SYSTEM FOR COMPUTER-ASSISTED ANTERIOR CRUCIATE LIGAMENT SURGERY", MEDICAL IMAGE ANALYSIS, OXFORD UNIVERSITY PRESS, OXOFRD, GB, vol. 3, no. 3, 1 September 1999 (1999-09-01), pages 209-222, XP008067851, ISSN: 1361-8415**
- **NOETZLI H P ET AL: "The contour of the femoral head-neck junction as a predictor for the risk of anterior impingement", JOURNAL OF BONE AND JOINT SURGERY. BRITISH VOLUME, LIVINGSTONE, LONDON, GB, vol. 84B, no. 4, 1 May 2005 (2005-05-01), pages 556-560, XP008157466, ISSN: 0301-620X cited in the application**

Printed by Jouve, 75001 PARIS (FR)

(Cont. next page)

- Lopes D. S., Jorge j. P., Pires E.B., Simões F. M. F.: "A three-dimensional geometric model of a hip joint presenting a femoral head deformity based on radial magnetic resonance arthrography images", VIPIMAGE 2009 - II ECCOMAS Thematic Conference on Computational Vision and Medical Image Processing, Porto, Portugal , 14 October 2009 (2009-10-14), XP008158740, Retrieved from the Internet: URL:https://dspace.ist.utl.pt/bitstream/2295/639639/2/lopatd.pdf [retrieved on 2012-10-12]
- PISE U V ET AL: "A B-spline based heterogeneous modeling and analysis of proximal femur with graded element", JOURNAL OF BIOMECHANICS, PERGAMON PRESS, NEW YORK, NY, US, vol. 42, no. 12, 25 August 2009 (2009-08-25), pages 1981-1988, XP026446859, ISSN: 0021-9290 [retrieved on 2009-06-21]

Description

TECHNICAL FIELD:

[0001] The invention relates to the field of computer assisted surgery, and more particularly to a method for determining bone resection on a deformed articulation surface.

BACKGROUND OF THE INVENTION:

[0002] Articulations of the human body are often very complex systems and no precise generic model exists to capture all the variability from one articulation to another. It is therefore necessary to use specific medical images or collection of digital patient data in order to get relevant information to develop techniques, devices and methods that will facilitate a treatment or a diagnosis.

[0003] In a specific example related to the hip articulation, structural abnormalities in the morphology of the hip can limit motion and result in repetitive impact of the proximal femoral neck against the acetabular labrum and its adjacent cartilage. Femoro Acetabular Impingement (FAI) is a pathology that can result from a decreased femoral head-neck offset (cam effect), an overgrowth of the bony acetabulum (pincer effect), excessive acetabular retroversion or excessive femoral anteversion, or a combination of these deformities. The cam impingement is generally characterized by a bone overgrowth located at the antero-superior aspect of the femur head-neck junction, which destructures the spherical shape of the femur head. The pincer impingement is generally characterized by an overcoverage located at the anterior aspect of the acetabulum rim. However, the correct and full diagnosis of this pathology is not easy to determine, especially when dealing with subtle deformities. Standard radiographic X-rays are used for the initial diagnosis and then three dimensional (3D) Computed Tomography (CT) scans or Magnetic Resonance Imaging (MRI) exams are generally performed in case of suspected FAI pathology. The processing of the 3D images remains a laborious manual task which cannot ensure accuracy and reproducibility, potentially misleading the diagnosis or the surgical indication. Moreover, even though 3D information can be extracted from such exams, the reconstructed bone volumes remain static and cannot predict with reliability the exact location of the impingement which occurs during the mobilization of the hip.

[0004] The surgical treatment of FAI aims at restoring a normal spherical shape to the femur head neck junction at the level of the bony cam lesion and restoring a normal coverage rate of the acetabular rim at the level of the pincer lesion, by removing the excess of bone. The result of this bony reshaping is the restoration of a greater range of motion of the hip, without impingement. Conventionally, the open surgical approach had initially been adopted since it provides a full exposure of the bone and direct access to the anatomy to be treated. Though, since minimally invasive procedures have grown in popularity by reducing the pain, morbidity and recovery time for patient, arthroscopic treatment of FAI has been explored in the last decade, which requires the use of an endoscopic camera and specific small instruments that can pass through various types of canulas. Advantages include minimally invasive access to the hip joint, peripheral compartments, and associated soft tissues. Furthermore, arthroscopy allows for a dynamic, intra-operative assessment and correction of the offending lesions. However, due to the depth of the joint and the reduced visibility and access, theses hip arthroscopy procedures are difficult to perform and not all surgeons feel comfortable about adopting the technique. The success of such arthroscopic interventions relies on correct diagnosis, accurate pre-operative assessment of the pathology, very meticulous intra-operative evaluation and a thorough and accurate correction of impingement lesions on both the femoral and acetabular sides, which can only be accomplished after a laborious learning curve over many cases. Failure of arthroscopic procedures for FAI is most commonly associated with incomplete decompression of the bony lesions.

[0005] Hence, one important issue is the difficulty to determine precisely and in a reproducible manner the location and amount of bone to be resected on a deformed articulation bone surface in order to recreate a smooth bone surface. The surgeons are generally applying 2D templates over the patient X-ray images to try to estimate the resection to be achieved. This remains a very limited and inaccurate method for addressing a problem in 3D space. The acquisition of a pre-operative 3D image of the patient is becoming a common protocol in these pathologies, thus increasing the level of information of the surgeon on the pathological problem. However, there are very few tools to process these 3D images and use resulting information in order to provide a proposition for the bone correction to be performed. Most of the imaging systems used to acquire the 3D images provide 3D reconstruction of bone surface models, however, the processing have to be applied manually and the results are only static projection views of the bone models. There exists some software proposing to simulate the resection pre-operatively, like the Mimics® software from Materialise, Leuven, Belgium, but the tools they offer are only simulation of bone milling process to be applied manually by the user, point by point, which takes a lot of time to perform, and does not guarantee reproducible results based on objective criteria. Another method consists in using the opposite side of the patient and mirror the opposite surface to define an optimal correction surface on the deformed side, but accurate results cannot be provided if the opposite side has also some early stage of deformity.

[0006] The characterization of the bone deformation by a so-called "alpha angle" measured on slice of the 3D image passing by the neck axis and quantifying the bump deformation on the head neck junction by a deviation

measure from an ideal sphere has been described by Nötzli et al ("The contour of the femoral head-neck junction as a predictor for the risk of anterior impingement", The Journal of Bone and Joint Surgery, Vol. 84B, No. 4, May 2002). Some methods have been developed to determine the resection to be applied to correct the deformation by removing the excess of bone which deviates from the ideal sphere (Kang et al, "Computer-assisted pre-operative planning for hip joint-preserving surgery", 5th Annual Meeting of the International Society for Computer Assisted Orthopaedic Surgery, Pro Business, pp. 212-214, June 2005; and Tannast et al, "Computer-assisted simulation of femoro-acetabular impingement surgery", in Navigation and MIS in Orthopaedic Surgery, Springer, pp. 440-447, 2007). US2007/0249967 A1 discloses a method for determining a patch surface from an impingement zone on a 3D surface bone model, said patch surface corresponding to an objective to be reached by the surgeon.

[0007] However a precise parameterization of the boundary of the targeted correction and the shape of the corrected bone surface has not been provided yet. One difficulty is to minimize the number of parameters defining such correction while ensuring to provide a valid correction covering individual specificities of the deformation.

[0008] In particular, obtaining a smooth transition and a minimal indentation for the new shape of the bone after correction has been formulated by several authors as reasonable and obvious criteria, but no method for efficient routine use has been proposed.

SUMMARY OF THE INVENTION:

[0009] The invention provides a method for non-invasive reproducible determination of a corrected surface on a 3D bone surface model constructed from 3D medical image of a bone having a deformation; the bone comprising a head portion contiguous to a neck portion, and the bone deformation consisting in a bump overgrowth at the head-neck junction, wherein said method comprises determining, from said 3D bone surface model, geometrical elements characterizing the anatomy of the bone, said geometrical elements including a sphere fitted to the spherical portion of the head and a neck axis,
wherein said corrected surface comprises :

i) a 3D spherical corrected surface patch on the head portion of said 3D bone surface model, and

ii) a 3D smooth transition corrected surface patch on the neck portion of said 3D bone surface model, contiguous to said 3D spherical corrected surface patch;

and wherein said corrected surface patches are defined by a set of parameters comprising:

iii) at least one first parameter (a *) representing a spherical extent value of said 3D spherical corrected surface patch, said first parameter (a *) being a target angle, expected to be achieved after surgery, measured radially between the hemi-line issued from the center of the fitted sphere and orientated distally along the neck axis, and a radius of the fitted sphere,
iv) and a set of at least one second parameter in addition to said first parameter, said set determining the 3D correction boundary of said corrected surface patches, said at least one second parameter defining the extent on the 3D bone surface model of said 3D correction boundary,

such that said 3D smooth transition corrected surface patch is continuous with said 3D bone surface model along said boundary, and such that the surface tangents to said 3D smooth transition corrected surface patch along said boundary are continuous with the surface tangents to said 3D bone surface model outside said boundary.

[0010] Embodiments of the invention are provided by the dependent claims.The embodiments and/or examples of the following description which are not covered by the appended claims are to be considered as not being part of the present invention.

[0011] Said set of parameters may advantageously consist consists of said first parameter and one second parameter.

[0012] The method may further comprise the following steps:

i) determining from said 3D bone surface model and from said geometrical elements characterizing the anatomy of the bone, a clock face referential on the head portion of the bone rotating around the neck axis;
ii) determining a 3D head-neck junction curve on the 3D bone surface model characterizing the head-neck junction of the bone around the clock face referential; and
iii) determining from said 3D head-neck junction curve a summit point characterizing the maximum of the bump deformation; said summit point being the point of said 3D head-neck junction curve closest to the apex point of the spherical portion of the head of the bone;

and wherein the 3D correction boundary proximally extends up to said summit point.

[0013] Besides the method may further comprise the following steps:

i) determining the parallel of latitude α^* of the fitted sphere;
ii) determining two radial hemi-planes containing the neck axis and passing respectively at the intersection of said parallel of latitude α^* and the 3D head-neck junction curve; the clock indices of these two hemi-planes on said clock face referential determin-

ing a correction clock interval;

iii) determining on the 3D bone surface model a closed contour around said summit point of the 3D head-neck junction curve, which contour extends at least distally to the parallel of latitude α^*, and covers at least radially the correction clock interval, said closed contour being the 3D correction boundary;

[0014] According to an embodiment of the invention, the closed contour on the 3D bone surface model defining the 3D correction boundary consists of the intersection of the 3D bone surface model with a 3D boundary box, said 3D boundary box being a geometrical 3D construction defined from at least the second parameter.

[0015] In particular, said 3D boundary box may be a polyhedron.

[0016] According to an embodiment, said polyhedron is a geometrical construction delimited by the following four limits:

i) a proximal limit defined by a portion of the intersection of the 3D bone surface model with a plane orthogonal to the neck axis and passing through the summit point of the 3D head-neck junction curve included in the correction interval;

ii) two radial limits defined by the two bone contours defined respectively as the intersection of the 3D bone surface model by the two hemi-planes determining the correction clock interval;

iii) a distal limit defined by a 3D neck curve defined as the intersection of the 3D surface model by a plane orthogonal to the neck axis; the coordinate position along the neck axis defining a proximal point being the at least second parameter and which is located further down in the neck direction at a distance of at least the fitted sphere radius from the fitted sphere center;

the 3D correction boundary being fully determined from the couple of parameters (α^*, proximal point).

[0017] According to an er embodiment, said set of at least one second parameter includes two adjustable clock indices controlling the extent of the correction clock interval; wherein the two radial hemi-planes corresponding to these two indices produce new intersection contours with the 3D surface model, the radial limits of the 3D correction boundary being constituted by said new intersection contours; the 3D correction boundary being fully determined from the quartet of parameters (α^*, proximal point, first clock index, second clock index).

[0018] According to another embodiment, said set of at least one second parameter includes an adjustable distal point on the neck axis determining a distal adjustable plane orthogonal to the neck axis and intersecting the 3D surface model on the distal portion of the femoral neck, thus producing a new distal limit; the adjustable distal point being positioned between the coordinate on the neck axis of the plane passing through the parallel of latitude α^* and a predefined max distal coordinate on the neck axis; the 3D correction boundary being fully determined from the triplet of parameters (α^*, proximal point, distal point).

[0019] According to another embodiment, said set of at least one second parameter includes any of the set of adjustable parameters as described above; which combination controls the extent of the 3D correction boundary; the 3D correction boundary being fully determined from the set of 5 parameters being (α^*, proximal point, distal point, clock index 1, clock index 2).

[0020] The 3D boundary box may be a cylinder constructed by the following steps:

i) determining a summit radial hemi-plane passing through the neck axis and said summit point of the 3D head-neck junction curve;

ii) determining a radius line of the fitted sphere passing at the intersection of said summit radial hemi-plane and the parallel of latitude α^*;

iii) positioning the cylinder so that its long axis is along the defined radius line;

iv) determining the diameter of the cylinder so that the intersection curve of the external wall of the cylinder with the 3D surface model extends to cover the clock interval and the summit point.

[0021] Said set of at least one second parameter may include an adjustable axis vector, an adjustable axis issue point and an adjustable cylinder radius which determine respectively the orientation, position and size of said cylinder; said axis vector being adjustable from the initial radius line rotating around the center of the fitted sphere and with a predefined 3D angle variation; said axis issue point being adjustable along the neck axis in an interval between the center of the fitted sphere and the coordinate point on the neck axis of the orthogonal plane passing through the parallel of latitude α^*; the 3D correction boundary being fully determined from the quartet of parameters (α^*, axis vector, axis issue point, cylinder radius).

[0022] According to another embodiment, the 3D boundary box is a cone constructed by the following steps:

i) determining a summit radial hemi-plane passing through the neck axis and said summit point of the 3D head-neck junction curve;

ii) determining a radius line of the fitted sphere passing at the intersection of said radial hemi-plane and the parallel of latitude α^*;

iii) positioning the cone so that its rotational axis is along said radius line and issued from the center of the fitted sphere;

iv) determining the aperture angle of the cone so that the intersection curve of the external wall of the cone with the 3D surface model extends to cover the clock interval and the summit point.

[0023] Said set of at least one second parameter may include an adjustable axis vector, an adjustable axis issue point and an adjustable aperture angle which determine respectively the orientation, position and aperture of the cone; said axis vector being adjustable from the initial radius line rotating around the center of the fitted sphere and with a predefined 3D angle variation; said axis issue point being adjustable along the neck axis in an interval between the center of the fitted sphere and the coordinate point on the neck axis of the orthogonal plane passing through the parallel of latitude α^*; the 3D correction boundary being fully determined from the quartet of parameters (α^*, axis vector, axis issue point, aperture angle).

[0024] The determination of the 3D spherical corrected surface patch and the 3D smooth transition corrected surface patch within the 3D correction boundary comprises the steps of:

i) splitting the 3D correction boundary in two contiguous regions by the parallel of latitude α^*, one distal region on the neck side and one proximal region on the head side, a portion of the parallel of latitude α^* forming a common boundary between said two contiguous regions;
ii) determining the 3D spherical corrected surface patch inside the proximal region as a pure spherical portion of the fitted sphere;
iii) determining the 3D smooth transition corrected surface patch inside the distal region by a 3D transition surface spline, said 3D transition surface spline being continuous with the 3D spherical corrected surface patch inside the proximal region along the common boundary, and continuous with the 3D bone surface model along its other boundary;

the union of the 3D spherical corrected surface patch and the 3D smooth transition corrected surface patch constituting a 3D corrected surface inside the 3D correction boundary.

[0025] Advantageously, the surface tangents of said 3D transition surface spline are continuous with the surface tangents of the 3D spherical corrected surface patch along the common boundary, and the surface tangents of said 3D transition surface spline are continuous with the surface tangents of the 3D bone surface model along its other boundary.

[0026] The 3D spherical corrected surface patch may further be determined by a 3D spherical surface spline, said 3D spherical surface spline being continuous with the 3D smooth transition corrected surface patch along the common boundary and continuous with the 3D bone surface model along its other boundary, and wherein the surface tangents of the 3D spherical corrected surface patch are the tangents of the fitted sphere along the common boundary and the surface tangents of the 3D spherical corrected surface patch are continuous with the tangents of the 3D bone surface model along its other boundary.

[0027] The surface tangents of said 3D transition surface spline along the common boundary may further be adjustable by a radial vector field controlling the surface tangents of said 3D transition spline surface along the common boundary to adjust the curvature at the junction of 3D spherical corrected surface patch and the 3D smooth transition corrected surface patch; all vectors of said radial vector field being issued from regular points located on the common boundary and being orientated towards a point on the neck axis located in the interval from the center of the fitted sphere to a predefined maximum distal point on the neck axis; the adjustable orientation of the vector field towards the center of the femoral head resulting in the emergence of a sharp edge in said 3D corrected surface patch, along the common boundary.

[0028] The length of the radial vector field can also be adjusted to control the height of said emerging sharp edge.

[0029] The boundary of the distal region may be composed of the two following portions:

i) the common boundary, and
ii) an external distal boundary being the boundary of the distal region minus the common boundary;

wherein the 3D transition surface spline is constructed from surface interpolation between a set of radial 3D Bezier curves of degree at least 3, located at regular clock intervals on the clock correction interval.

[0030] Each of the radial 3D Bezier curve may be determined by a distal extremity control point located on the 3D bone surface model along the external distal boundary, and a proximal extremity control point located on the fitted sphere along the common boundary.

[0031] Each of the radial 3D Bezier curve slope may be determined by a distal slope control point located on the 3D bone surface model, shifted proximally by a predetermined coefficient in the direction of the neck axis from the distal extremity control point, and by a proximal slope control point located at the end point of the radial vector of the corresponding radial index.

DESCRIPTION OF THE DRAWINGS:

[0032] Further aims, features and advantages of the invention will appear in the following detailed description with reference to illustrative and non limitative drawings, among which:

Fig.1 is a representation of the different steps being carried in the method, illustrating the initial input and the final output.
Fig. 2A shows two orthogonal 2D images extracted from the 3D image, in axial and coronal direction, commonly used to determine manually the position the femoral head sphere and the neck axis.

Fig. 2B shows a perspective view of a reconstructed 3D surface model of the bone, with a sphere fitted to the head portion and a neck axis.

Fig. 3 is a 2D image extracted from the 3D image at the level of the knee, commonly used to determine the knee center point;

Fig. 4A and 4B show perspective views of the femur illustrating the determination of the clock face referential on the femoral head;

Fig. 5 is a perspective view of the proximal femur showing the 3D head-neck junction curve at the intersection of the femoral head surface and the femoral head sphere model;

Fig. 6 shows a cross-sectional view of the proximal femur along the femoral neck axis illustrating the determination of the femur surface points composing the 3D head-neck junction curve;

Fig. 7 shows a zoomed cross-sectional view of the proximal femur illustrating the selection in a radial hemi-plane of the point where the bone surface first deviates from the femoral sphere, within a predefined threshold distance.

Fig. 8 shows a perspective view of the proximal femur illustrating the characterization of the summit of the bump deformation on the 3D head-neck junction curve by a clock index and a max alpha angle.

Fig. 8 is a perspective view of the proximal femur showing the determination of the spherical correction on the head portion and a smooth junction correction on the neck within a correction boundary.

Fig. 9A is a perspective view of the proximal femur showing the determination of a parallel of latitude of desired angle, proximal to which the corrected surface is a spherical portion surface and distal to which the corrected surface is a smooth transition to the neck portion.

Fig. 9B is a zoomed cross-sectional radial view of the proximal femur showing the determination of the spherical correction on the head portion and a smooth junction correction on the neck within a correction boundary.

Fig. 10A is a perspective view of the proximal femur showing the definition of a boundary box to determine the limits of the corrected surface.

Fig. 10B is a zoomed perspective view of the proximal femur showing the boundary curve resulting from the determination of the boundary box.

Fig. 11 is a perspective view of the proximal femur showing a boundary box determined by four planes and resulting in the full determination of the 3D correction boundary from two parameters only.

Fig. 12 is a perspective view of the proximal femur illustrating four additional parameters which can be used to control the 3D correction boundary.

Fig. 13A and 13B are respectively zoomed cross-sectional radial and axial views of the proximal femur illustrating the full control of the 3D correction boundary and the 3D shape of the corrected surface by a five parameters.

Fig. 14 is a perspective view of the proximal femur illustrating the determination of the 3D correction boundary its border curves from the parameterization of the 3D correction boundary its border by the five parameters of Fig. 13A and 13B.

Fig. 15A illustrates the determination of the 3D boundary box as a cylinder;

Fig. 15B illustrates the determination of the 3D boundary curve on the 3D bone surface resulting in the intersection of the cylinder described in Fig. 15A with the 3D bone surface;

Fig. 16A illustrates the determination 3D boundary box as a cone;

Fig. 16B illustrates the determination of a 3D boundary curve on the 3D bone surface resulting in the intersection of the cone described in Fig. 16A with the 3D bone surface;

Fig. 17A is a perspective view of the proximal femur illustrating the determination of the 3D corrected surface patches using 3D surface spline models.

Fig. 17B is a zoomed view on a point on the 3D surface spine model at the junction of the spherical corrected surface patch and the smooth transition corrected surface patch, illustrating the continuity between the surface and surfaces tangents of both patches.

Fig. 17 is a radial cross-sectional view of the proximal femur illustrating an additional parameter used to control the edge of 3D shape of the correct surface along the junction between the spherical portion and the smooth neck surface portion.

Fig. 18A is a perspective view of the proximal femur illustrating the construction of the 3D surface spline of the smooth transition corrected surface patch using surface interpolation between a set of radial 3D Bezier curves.

Fig. 18B is a zoomed cross-sectional radial view illustrating the construction of the 3D Bezier curve from Bezier control points in one radial hemi-plane.

Fig. 19A and 19B are respectively zoomed cross-sectional radial and axial views of the proximal femur illustrating the use of other parameters to control the surface curvature at the junction of the 3D spherical corrected surface patch and the 3D smooth transition corrected surface patch.

DETAILED DESCRIPTION OF THE INVENTION:

[0033] The method described hereafter provides a precise and reproducible process to determine from 3D medical image of the bone, a correction of a bone deformation at the head-neck junction of the bone, with a limited number of parameters, enabling an individual adjustment of the correction boundary and corrected shape.

[0034] In reference to the drawings, a method for non-invasive determination of parameters defining a boundary and a corrected surface from a resection of a de-

formed surface of a bone is hereafter described. The resection of a deformed surface of the bone is used for correction of an articulation condition.

[0035] In the following description, the method is described with reference to the hip articulation. Thus, the method will be used for defining a resection of a bump overgrowth deformed surface on the femur head neck junction. However, the invention is not limited to the application to the femur but can be used for defining a resection of a deformed surface of any articulation bone comprising a head and a neck. The person skilled in the art will easily adapt the method of the invention to such articulation bones.

[0036] As shown in figure 1, the method requires a 3D image examination of the patient acquired using a specific predefined protocol. For example, 2D images of the hip can be acquired to construct the 3D image by computer tomography (CT): the 2D images are parallel one with the other and are stacked, creating the 3D image. In addition to the conventional 3D image acquisition protocol for the hip, few extra CT images at the level of the knee are also acquired.

[0037] In a first preliminary step PS1 the 3D image of the hip is processed for extracting critical geometrical elements characterizing the femur. These geometrical elements can be determined interactively by the user using standard orthogonal 2D images extracted from the 3D image as illustrated in FIG. 2A, such orthogonal 2D images being determined by sliding along an axial direction and a frontal direction in the 3D image volume to select the images showing the best view of the searched geometrical elements. In the present example, the required geometrical elements are a femoral head sphere SF fitting the non-deformed part of the femoral head, a femoral head center point H, center of the sphere SF, a femoral neck axis AX, and a knee center point K.

[0038] As illustrated in FIG. 2A, the sphere SF is determined by placing interactively a circle on the femur head contours in at least two orthogonal 2D images extracted from the 3D image in axial and coronal directions. The size and position of the femoral head sphere SF is interactively adjusted, which results in the determination of the 3D femoral head sphere SF. The femoral head center H is then determined as the center of the femoral head sphere SF. The neck axis AX is determined by interactively placing a vector line passing through the middle of the femur neck axis in the orthogonal 2D images. The knee center K is determined by interactively placing a point in the most distal 2D images extracted from the 3D image corresponding to the center of the knee.

[0039] In a variant embodiment illustrated in FIG. 3B, the knee center K is determined by placing interactively two points E1 and E2 corresponding to the epicondyles defined as the most lateral and most medial points of the knee. The knee center K is then determined as the middle of the segment [E1E2].

[0040] In a second preliminary step PS2, a 3D bone surface model of the deformed bone surface is constructed from the 3D image as illustrated in FIG. 2B. In the case of CT image, step PS2 is commonly carried out with a thresholding process. Additional processing using well known mathematical morphology operators is applied to eliminate small connected components, such as erosion and dilation, and to fill the inside of surfaces so that only external surfaces of the bone remain. The femoral head sphere SF, the femoral head center H and the neck axis AX can then be represented on the 3D bone surface model.

[0041] In further description, the anatomical directions are defined as follows:

[a] superior-inferior direction is orientated vertically from the head center H to the knee center K;
[b] and proximal-distal direction is orientated along the neck axis, from the head center H down towards the neck.

[0042] In a third preliminary step PS3, a clock face referential on the femur head, around the neck axis AX is determined. The clock face is a radial referential system representing twelve hour angular segments rotating around the neck axis AX, commonly used by surgeons to identify location of points on the bone head surface. The clock face is entirely defined by determination of a 12 o'clock position 12h. This 12 o'clock position 12h is determined from a plane P12h passing through the neck axis AX and the knee center point K as shown in FIG. 4A. The 12 o'clock position 12h is defined by the hemi-plane P12h that is the superior half of the plane P12h farthest from the knee, the other inferior half of the plane P defining the location of a 6 o'clock position 6h. Successive rotations of 30° of this hemi-plane P12h around the neck axis AX in the anterior direction will then define a 1 o'clock position, 2 o'clock position, 3 o'clock position, and so on until full quadrant is determined. FIG. 4B illustrates this construction. In a similar manner, successive rotations of 15° will define half-hour clock positions. Still in a similar manner, successive rotations of 7.5° will define quarter-hour clock positions. Further precision on the clock face is not sought for since further precision is irrelevant for the practitioner who cannot be as precise. However, in case the surgery is automated, further precision can be helpful and the clock face is further divided into five-minute clock positions or even 1-minute clock positions. The clock face thus partitioned determines a clock face referential.

[0043] Once the clock face has been determined on the femur, the location and extent of the deformed bone overgrowth is determined by overlaying the femoral head sphere SF, centered on the femoral head center H, on the 3D bone surface model in a forth preliminary step PS4. The overlay can be implemented using transparency effects, color maps of distances, or simply wire mesh for one of the femoral head sphere SF or 3D bone surface model and facets mesh for the other. The intersection of the sphere SF and the 3D bone surface model

determines a 3D head-neck junction curve showing the extent of the deformed bone overgrowth area. As illustrated in FIG. 5, this 3D head-neck junction curve can be approximated by linking a succession of points Mi, each points Mi being defined within a radial hemi-plane of the clock face and indexed by a clock index i in the clock face referential and. As shown in FIG. 6, each Mi point is determined in the radial hemi-plane Pi of clock index i, such that it characterizes the location of the deviation of the bone surface from the sphere SF, thus determining an angle alpha αi measured as the angle between the neck axis AX and the radius (HMi).

[0044] As the 3D surface model may present some micro-local deformations which are not intented to be taken into account in the resection of the deformed surface, the points Mi are determined as the bone surface points located just above the surface of the sphere SF, beyond a given threshold TD.

[0045] The zoomed view of FIG. 7 illustrates the selection of a point Mi amongst a plurality of candidate points Mij (j being an integer of an index position of an angle between 0° and 180°) in the same hemi-plane Pi, the distances between a candidate points Mij and the femoral head sphere SF surface is determined in the direction of the radius HMij. The candidate points Mi1, Mi2, from which the 3D surface model extends outside the femoral head sphere SF but only beneath the given threshold TD are discarded. The candidate point Mi3, from which the 3D surface model extends outside the femoral head sphere SF beyond the given threshold TD is selected. The value of the threshold TD is arbitrarily fixed depending on the noise of segmentation process. The value of the threshold TD is typically 0.5 mm or 1 mm. The 3D curve created by the selected points Mi defines the limit from which the femoral head loses its sphericity and where the deformed bone overgrowth starts. Each point Mi is associated with its corresponding hemi-plane Pi passing through the neck axis AX and the point Mi, and its clock index i. Then, as illustrated in FIG. 8 the point Mmax for which the alpha angle αmax is greatest is determined, the clock index iMax of which is also registered. The point Mmax defining the summit of the deformed bone surface on the 3D head-junction curve.

[0046] The resection of the deformed bone surface can then be determined from a main criterion which is to decrease the value of α max to a target alpha angle α*, by simulating the resection of the deformed bone overgrowth. This determines a corrected bone surface that will increase the spherical portion of the femoral surface and creates a smooth transition surface to non-corrected areas in the direction of the neck.

[0047] In a preferred embodiment, a first parameter is the correction target alpha angle α*, that is expected to be obtained post-operatively, after the bone correction. It represents the degree of sphericity that the corrected femoral head should have.

[0048] As illustrated in FIG. 9A and 9B, this parameter α* defines a parallel L* of latitude α* on the surface of the sphere SF, α* being the angle measured between the neck axis and any radius line issued from the center H of the sphere SF passing by the parallel L*. The corrected surface on the proximal side, closest to the head, of the parallel L* is then determined as a pure spherical surface portion SP1 of the sphere SF, extending proximally at least to the summit Mmax and radially at least to two clock indices i and j corresponding to most distant clock positions on each side of Mmax for which the respectively measured angles αi and αj are equal to α*, and which distal border is defined by the parallel L*, SP1 determining a 3D spherical corrected surface patch.

[0049] Apart from restoring sphericity to the femoral head, the invention also intends to provide a smooth transition corrected surface between the 3D spherical corrected surface patch and the non-corrected surface of the neck portion. By "smooth transition" is meant that the corrected surface is extended from the border of the parallel L* in the direction of the neck in order to provide a corrected surface flush to the non-corrected 3D bone surface model without sharp edges and restoring the curvature of the neck. From all the curves and surfaces defined so far, it is possible to use a conventional Computer Aided Design software package like Pro-Engineer or SolidWorks to build interactively spline patches in order to generate the 3D smooth transition corrected surface. This will implement the requirement of having a smooth transition and a minimal indentation for the new shape of the bone after correction, which has been formulated by several authors as reasonable and obvious criteria, However, this cannot be accomplished easily, it requires specialized technical skills and a lot of time. A challenge of the invention is to provide a method to generate such spline patches automatically from just a set of a few parameters that can be adjusted manually or defined automatically as well. A related difficulty is to maintain a reasonable meaning associated to such parameters for a user that has no technical expertise such as a surgeon.

[0050] As illustrated in FIG. 9A and 9B, the distal extent of the smooth transition corrected surface is determined by a second parameter NO which is a coordinate position on the neck axis AX defining a plane orthogonal to the neck axis AX and creating a limit between the smooth transition corrected surface and the non-corrected 3D bone surface model. The position NO is determined arbitrarily from empirical knowledge of the anatomy, as for example to be at a distance of twice the radius of the sphere SF from the center H. Such smooth transition corrected surface is provided by a 3D smooth transition corrected surface patch SP2 that is continuous to the 3D spherical corrected surface patch SP1 and flush to the non-corrected 3D bone surface model of the neck portion.

[0051] In order to fully determine the surface patches SP1 and SP2, the invention also provides methods to determine the boundary in which the correction is applied as described hereafter.

[0052] As illustrated in FIG. 10A and FIG. 10B, in a

preferred embodiment, a 3D boundary box BB intersects the femur head neck junction surface, thus defining a 3D boundary curve BC on the 3D bone surface model. The 3D boundary curve BC is split into two by the parallel L*, determining one proximal boundary PB which defines the limit of the 3D spherical corrected surface patch SP1, and one distal boundary DB which defines the limit of the 3D smooth transition corrected surface patch SP2, the boundaries PB and DB having a common portion LB supported by the parallel L*, their respective other boundary being the portion of respectively PB and DB without the portion LB. One intent of the invention is to provide parameters defining a construction of a 3D boundary box determining the proximal boundary PB and the distal boundary DB.

[0053] In a preferred embodiment illustrated by FIG. 11, the boundary box BB is determined by four planes delimiting a portion of the 3D bone surface model in the head neck junction area.

[0054] In a preferred embodiment, these four planes are fully determined from the first parameter α^* and the second parameter NO in the following manner:

[a] a proximal plane PN1 is determined as a plane orthogonal to the neck axis AX and passing through the summit point Mmax;
[b] a distal plane PN0 is determined as a plane orthogonal to the neck axis AX and passing at the coordinate value of the parameter NO on the neck axis;
[c] two radial hemi-planes Pi and Pj around the neck axis and passing at the clock indices i and j defined previously.

The intersection of these four planes with the 3D bone surface model determines the 3D correction boundary in which the corrected surface patches SP1 and SP2 are determined.

[0055] In another preferred embodiment, as illustrated in FIG. 12, these four planes are adjustable and their positions are determined from other parameters of the invention, enabling the adjustment of their positions, as illustrated in the radial cross-sectional view around the neck axis of FIG. 13A and in the axial cross-sectional view orthogonal to the neck axis of FIG 13B, in the following manner:

[a] the position of the proximal plane PN1 is adjustable according to the adjustable position of the coordinate point N1 on the neck axis,
[b] the position of the distal plane PN0 is adjustable according to the adjustable position of the coordinate point NO on the neck axis,
[c] the position of the two radial hemi-planes Pi0 and Pi1 are adjustable respectively according to the adjustable position of the clock indices i0 and i1 on the clock face referential;

[0056] The five parameters α^*, i0, i1, NO and N1, completely define the 3D correction boundary in order to obtain a desired degree of sphericity α^* and a smooth transition to the neck. The corrected bone surface is composed of the proximal surface patch SP1, which is spherical, and the distal surface patch SP2, which is a 3D smooth transition surface. The proximal and distal patches are determined by the boundary curve BC comprising four 3D edge curves and the boundary LB defined from the parallel L*, as illustrated in FIG 14 and defined as follows:

[A] the intersection curve Si0 between the plane Pi0 and the femur bone surface is the first clock extent edge;
[B] the intersection curve Si1 between the plane Pi1 and the femur bone surface is the second clock extent edge;
[C] the intersection curve SN0 between the plane PN0 and the femur bone surface is the distal edge;
[D] the intersection curve SN1 between the plane PN1 and the femur bone surface is the proximal edge; and
[E] the boundary curve LB defined from the parallel L* corresponding to the target alpha angle α^*.

[0057] In another preferred embodiment, the boundary box BB is determined by a right circular cylinder, as illustrated in FIG. 15A. The cylinder is defined by a long axis orthogonal to the neck axis AX, and a diameter of the circular base of the right circular cylinder. The long axis of the cylinder is positioned so that the wall of the right circular cylinder is tangent to the point Mmax previously determined. The diameter of the cylinder base Dc determines a parameter of the boundary box BB, which preferred value is equal to the diameter of the femoral head sphere described earlier. For that embodiment, the boundary curve BC defines a smooth 3D skew curve with no sharp edges as illustrated in FIG. 15B. The same construction of the spherical surface patch SP1 and the smooth transition surface patch SP2 as described above is applied with the definition of the new boundary curve BC. Hence, the two parameters α^* and the diameter of the cylinder base Dc define completely the corrected bone surface in order to obtain a desired degree of sphericity α^* and a smooth transition to the neck. Other parameters can be added to control the orientation and position of the axis of the cylinder.

[0058] In a similar manner, in another preferred embodiment illustrated in FIG. 16A, the boundary box BB is determined by a solid cone, the size and position of which are determined as follows. The cone has an axis, which is determined by the radius line of the femoral head sphere SF corresponding to the target angle α^*, and comprised in the plane PMax earlier determined. The solid angle β of the cone determines a parameter of the boundary box BB, which preferred value is chosen such that the point Mmax is inside the cone. Again, as illustrated in FIG. 16B, the boundary curve BC defines a smooth

3D skew curve with no sharp edges. The same construction of the spherical surface patch SP1 and the smooth transition surface patch SP2 as described above is applied with the definition of the new boundary curve BC. Hence, the two parameters α^* and solid angle β of the cone completely define the corrected bone surface in order to obtain a desired degree of sphericity α^* and a smooth transition to the neck. Other parameters can be added to control the orientation and the axis of the cone.

[0059] In similar manner, any type of geometrical volume for which the position and size can be parameterized relatively to the 3D bone surface model or specific anatomical landmarks can define a bounding box BB, the intersection of which with the 3D bone surface model results in a boundary curve BC. The surface determined by this boundary curve BC is parted into two portions by the parallel L*, which defines the degree of sphericity of the corrected bone surface. Inside the proximal boundary, the 3D corrected surface is a spherical surface patch, and inside the distal boundary, the 3D corrected surface is a smooth transition surface patch. The desired degree of continuity can be defined on each boundary edge.

[0060] As illustrated in FIG. 17A, once the 3D correction boundary has been determined, the surface patches SP1 and SP2, can be fully determined, the 3D spherical corrected surface patch SP1 describing a portion of the sphere SF inside the proximal boundary PB and the 3D smooth transition corrected surface patch SP2 describing a surface inside the distal boundary DB, the common boundary LB between both surface patches being supported by the parallel L* of latitude α^*.

[0061] In a preferred embodiment, the surface patch SP2 can be constructed for example from a 3D surface spline model, such that SP2 is continuous with SP1 and SP2 surface tangents are continuous with SP1 surface tangents along the common boundary LB. This continuity of surface and surface tangents is illustrated in the zoomed view of FIG. 17B at the location of a point CBk of the 3D surface spline of the surface patch SP2 on the common boundary LB. The continuity is carried out at each point CBk by imposing local constraints on the 3D surface spline such that the surface points CBk are located on the boundary LB, and that surface tangent vectors V2x and V2y of the 3D surface spline are parallel respectively to the surface tangent vectors V1x and V1y of the spherical surface patch SP1 and orientated in the opposite direction It is easily understood from the man of the art that this construction of the 3D surface spline along the boundary LB can be transposed to the other points of the distal boundary DB, such that the 3D surface spline is continuous at each point DBj with the external 3D bone surface model ES, and the surface tangents of the 3D surface spline are continuous at each point DBj with the surface tangents of the external 3D bone surface model ES. The distal surface patch SP2 is constructed for instance by using mathematical 3D surface patch models like Bezier surface spline models for example.

[0062] Optimally, in another preferred embodiment, since the femoral head surface outside the proximal boundary PB does not match perfectly the sphere SF, the proximal surface patch SP1 can also be determined from a 3D surface spline model so to control the surface continuity and the surface tangents continuity between SP1 and the external 3D bone surface model ES, along the proximal boundary PB. As previously exposed, it is easily understood from the man of the art that the construction of the 3D surface spline of the surface patch SP2 can be transposed for the construction of the 3D spline of the surface patch SP1, such that the 3D spline of the surface patch SP1 is continuous at each point PBi along the proximal boundary PB with the external 3D bone surface model ES, and the surface tangents of the 3D spline of the surface patch SP1 are continuous at each point PBi with the surface tangents of the external 3D bone surface model ES.

[0063] In a preferred embodiment where the 3D correction boundary is determined from a set of four planes as described previously, and as illustrated in FIG. 14, the proximal surface patch SP1 is determined as a portion of the sphere SF, limited by Si0, Si1, SN1 and LB. Along the limit LB, SP1 is continuous to the distal surface patch SP2 delimited by Si0, Si1, L* and SN0. The distal surface patch SP2 is a smooth surface that smoothly connects the proximal surface patch SP1 to the non-corrected part of the bone.

[0064] In a preferred embodiment, the proximal surface patch SP1 is continuous with the femur 3D bone surface at the edge curves Si0, Si1, SN, and the distal surface patch SP2 is continuous with the femur 3D bone surface at the edge curves Si0, Si1, SN0 and LB. Optimally, SP1 and SP2 can be determined with construction constraints such that the surface tangents are also continuous with the tangents to the femur 3D bone surface at the loci of the four edge curves Si0, Si1, SN0 and SN1. Optimally the distal surface patch SP2 tangents are also continuous with the surface tangent of the proximal surface patch SP1 at the locus of LB. Continuity of the second derivatives of the surfaces can also be a possible constraint to create very smooth transitions at the location of the 5 edge curves Si0, Si1, SN0, SN1 and LB. Several mathematical models of interpolation can therefore be used to define first and second portions SP1 and SP2 in order to meet these constraints.

[0065] In a preferred embodiment, and as illustrated in FIG. 18A, the distal surface patch SP2 is constructed by interpolating 3D surface spline models from a set of radial 3D Bezier curves BZi at regular intervals along the clock face referential. As illustrated in FIG 18B, each 3D Bezier curve BZi is defined in the hemi-radial plane Pi by four control points C1, C2, C3, C4 determined as follows:

[a] the proximal extremity control point C1 is positioned on the common boundary LB defined by the parallel L* of latitude α^*;

[b] the proximal tangent control point C2 is positioned so as to form with C1 a vector V2x parallel to the

tangent vector V1x of the spherical portion SP1 and in the opposite direction;

[c] the distal extremity point C4 is positioned on the 3D bone surface model along the distal boundary;

[d] the distal tangent control point C3 is positioned on the 3D bone surface model, shifted from the position of C4 proximally along the neck axis direction, by a predefined coefficient, such that the surface tangent vector V3x of the Bezier curve BZi at the location of the extremity point C4 is parallel to the surface tangent vector V4x of the 3D bone surface model and in the opposite direction;

[0066] To go further in the description of the 3D corrected surface, in some pathology cases, it can be important to deepen the 3D smooth transition corrected surface just below the junction with the 3D spherical corrected surface to increase the mobility of the femoral head into the socket bone. To enable this type of transition, in another preferred embodiment, another parameter of the method consists of a radial vector field issued from points on the common boundary LB at regular intervals, to control the slope of the 3D smooth transition corrected surface patch SP2 along the common boundary LB.

[0067] As illustrated on FIG. 19A and 19B, the radial vector field V* is constituted of the set of vectors V*i determined in radial hemi-planes Pi at regular intervals between the clock indices i0 and i1. All vectors Vi* are orientated towards a point of coordinate N2 on the neck axis, the set of vectors Vi* determining the surface tangents of the 3D corrected surface patch SP2 along the common boundary LB. When the coordinate N2 is adjusted along the neck axis, each vector Vi* deviates from the surface tangent V1x of the 3D spherical surface patch SP1, thus generating an edge in the 3D corrected surface, along the common boundary LB. In another embodiment, the length of the vectors Vi* of the radial vector field V* can also be another parameter to control the height of the edge along the common boundary LB.

[0068] In a preferred embodiment, the value of the parameter α^* is set to an arbitrary value such as 45° for example, which is a common target value used by surgeons, and other parameters are then defined automatically accordingly to the methods described above. The corrected bone surface is thus entirely determined automatically.

[0069] In another preferred embodiment, the value of the parameter α^* is determined from the sphericity of the femoral head measured on the opposite hip, from 3D medical image.

[0070] In another preferred embodiment, the value of the target alpha angle α^* parameter is defined interactively by the user in the range [25°; 90°] in order to obtain a more or less spherical extent of the corrected bone surface. All other parameters are then defined automatically and the corrected bone surface is thus entirely defined.

[0071] In another preferred embodiment, any of the parameters α^* and the other parameters defining the boundary box are defined interactively by the user in a predefined range, in order to obtain a more or less spherical extent of the corrected bone surface but also more or less extent along the neck axis and more or less extent around the clock.

[0072] In another preferred embodiment, any of the parameters α^* and the other parameters defining the boundary box and other parameters defining an edge at the junction of the spherical and smooth transition corrected surfaces are defined interactively by the user in a predefined range.

[0073] In a preferred embodiment, the determination of the corrected surface patches results in the computation of a percentage of resection volume in the neck-junction portion.

[0074] In another preferred embodiment, the determination of the corrected surface patches results in the computation of a restored offset value computed as the maximum of the distances determined in the hemi-radial planes of the correction clock interval as the distance between two straight lines parallel to the neck axis, one of the line passing through the highest point of the head contour, the other line passing at the lowest point of the corrected surface of the neck.

[0075] The method can be implemented in software running on a standard computer. The user can interact with the software by a standard user interface medium like a mouse, touch screen or the like. Images are displayed on the monitor of the computer. At the beginning, the software is used to select and load the 3D image of the specific patient.

[0076] The software is intended to determine the optimal corrected bone surface of a deformed articulation bone surface, the bone comprising a head and a neck.

[0077] In a preferred embodiment, the software is intended to determine the optimal corrected bone surface of a bump on a bone.

[0078] Description with the femur head-neck junction in the case of Femoro-Acetabular Impingement (FAI) is illustrative and easily adaptable for other bones with head-neck junction. Also, the method is detailed for 3D CT images but it can be extended to other 3D image modality as MRI for example.

ADVANTAGES:

[0079] The invention offers a method for easy, accurate and reproducible determination of a bone resection of a deformed bone surface. The proposed method is based on automatic determination of parameters values in order to determine the optimal resection. The method determines automatically the boundary of the bone area to be resected. The method also determines automatically a shape for the corrected surface respecting sphericity increase of the head of the bone and smooth transition at the neck of the bone. Simple user interaction over a limited number of parameters is possible to fine

tune or customize the proposal for the bone resection.

Claims

1. A method for non-invasive reproducible determination of a corrected surface on a 3D bone surface model constructed from 3D medical image of a bone having a deformation; the bone comprising a head portion contiguous to a neck portion, and the bone deformation consisting in a bump overgrowth at the head-neck junction, wherein said method comprises determining, from said 3D bone surface model, geometrical elements characterizing the anatomy of the bone, said geometrical elements including a sphere fitted to the spherical portion of the head and a neck axis,
wherein said corrected surface is **characterised by** comprising:

    i) a 3D spherical corrected surface patch on the head portion of said 3D bone surface model, and
    ii) a 3D smooth transition corrected surface patch on the neck portion of said 3D bone surface model, contiguous to said 3D spherical corrected surface patch;

    and wherein said corrected surface patches are defined by a set of parameters comprising:

    iii) at least one first parameter (α*) representing a spherical extent value of said 3D spherical corrected surface patch, said first parameter (α*) being a target angle, expected to be achieved after surgery, measured radially between the hemi-line issued from the center of the fitted sphere and orientated distally along the neck axis, and a radius of the fitted sphere,
    iv) and a set of at least one second parameter in addition to said first parameter, said set determining the 3D correction boundary of said corrected surface patches, said at least one second parameter defining the extent on the 3D bone surface model of said 3D correction boundary,

    such that said 3D smooth transition corrected surface patch is continuous with said 3D bone surface model along said boundary, and such that the surface tangents to said 3D smooth transition corrected surface patch along said boundary are continuous with the surface tangents to said 3D bone surface model outside said boundary.

2. The method of claim 1 wherein the set of parameters consists of said first and second parameters.

3. The method of claim 1 or claim 2, further comprising the following steps:

    i) determining from said 3D bone surface model and from said geometrical elements characterizing the anatomy of the bone, a clock face referential on the head portion of the bone rotating around the neck axis;
    ii) determining a 3D head-neck junction curve on the 3D bone surface model characterizing the head-neck junction of the bone around the clock face referential; and
    iii) determining from said 3D head-neck junction curve a summit point characterizing the maximum of the bump deformation; said summit point being the point of said 3D head-neck junction curve closest to the apex point of the spherical portion of the head of the bone;

    and wherein the 3D correction boundary proximally extends up to said summit point.

4. The method of claim 3, further comprising the following steps:

    i) determining the parallel of latitude α* of the fitted sphere;
    ii) determining two radial hemi-planes containing the neck axis and passing respectively at the intersection of said parallel of latitude α* and the 3D head-neck junction curve; the clock indices of these two hemi-planes on said clock face referential determining a correction clock interval;
    iii) determining on the 3D bone surface model a closed contour around said summit point of the 3D head-neck junction curve, which contour extends at least distally to the parallel of latitude α*, and covers at least radially the correction clock interval, said closed contour being the 3D correction boundary;

5. The method of claim 4 wherein the closed contour on the 3D bone surface model defining the 3D correction boundary consists of the intersection of the 3D bone surface model with a 3D boundary box, said 3D boundary box being a geometrical 3D construction defined from at least the second parameter.

6. The method of claim 5, wherein said 3D boundary box is a polyhedron.

7. The method of claim 6, wherein said polyhedron is a geometrical construction delimited by the following four limits:

    i) a proximal limit defined by a portion of the intersection of the 3D bone surface model with a plane orthogonal to the neck axis and passing through the summit point of the 3D head-neck

junction curve included in the correction interval;
ii) two radial limits defined by the two bone contours defined respectively as the intersection of the 3D bone surface model by the two hemi-planes determining the correction clock interval;
iii) a distal limit defined by a 3D neck curve defined as the intersection of the 3D surface model by a plane orthogonal to the neck axis; the coordinate position along the neck axis defining a distal point (N0) being the at least second parameter and which is located further down in the neck direction at a distance of at least the fitted sphere radius from the fitted sphere center;

the 3D correction boundary being fully determined from the couple of parameters (α*, distal point).

8. The method of claim 6, wherein said polyhedron is a geometrical construction delimited by the following four limits:

i) a proximal limit defined by a portion of the intersection of the 3D bone surface model with a plane orthogonal to the neck axis and passing through the summit point of the 3D head-neck junction curve included in the correction interval;
ii) two radial limits defined by the two bone contours defined respectively as the intersection of the 3D bone surface model by the two hemi-planes determining the correction clock interval;
iii) a distal limit defined by a 3D neck curve defined as the intersection of the 3D surface model by a plane orthogonal to the neck axis; the coordinate position along the neck axis defining a distal point (N0) being the at least second parameter and which is located further down in the neck direction at a distance of at least the fitted sphere radius from the fitted sphere center; and

wherein said set of at least one second parameter includes two adjustable clock indices controlling the extent of the correction clock interval; wherein the two radial hemi-planes corresponding to these two indices produce new intersection contours with the 3D surface model, the radial limits of the 3D correction boundary being constituted by said new intersection contours; the 3D correction boundary being fully determined from the quartet of parameters (α*, distal point, first clock index, second clock index).

9. The method of claim 6, wherein said polyhedron is a geometrical construction delimited by the following four limits:

i) a proximal limit defined by a portion of the intersection of the 3D bone surface model with a plane orthogonal to the neck axis and passing through the summit point of the 3D head-neck junction curve included in the correction interval; the coordinate position of the proximal limit on the neck axis defining a proximal point (N1);
ii) two radial limits defined by the two bone contours defined respectively as the intersection of the 3D bone surface model by the two hemi-planes determining the correction clock interval;
iii) a distal limit defined by a 3D neck curve defined as the intersection of the 3D surface model by a plane orthogonal to the neck axis; the coordinate position along the neck axis defining a distal point (N0) which is located further down in the neck direction at a distance of at least the fitted sphere radius from the fitted sphere center; and

wherein said set of at least one second parameter includes an adjustable distal point on the neck axis determining a distal adjustable plane orthogonal to the neck axis and intersecting the 3D surface model on the distal portion of the femoral neck, thus producing a new distal limit; the adjustable distal point being positioned between the coordinate on the neck axis of the plane passing through the parallel of latitude α* and a predefined max distal coordinate on the neck axis; the 3D correction boundary being fully determined from the triplet of parameters (α*, proximal point, distal point).

10. The method of any of claims 7 to 9 wherein said set of at least one second parameter includes any of the set of adjustable parameters defined in claims 9 or 10; which combination controls the extent of the 3D correction boundary; the 3D correction boundary being fully determined from the set of 5 parameters being (α*, proximal point, distal point, clock index 1, clock index 2).

11. The method of claim 5 wherein the 3D boundary box is a cylinder constructed by the following steps:

i) determining a summit radial hemi-plane passing through the neck axis and said summit point of the 3D head-neck junction curve;
ii) determining a radius line of the fitted sphere passing at the intersection of said summit radial hemi-plane and the parallel of latitude α*;
iii) positioning the cylinder so that its long axis is along the defined radius line;
iv) determining the diameter of the cylinder so that the intersection curve of the external wall of the cylinder with the 3D surface model extends to cover the clock interval and the summit point.

12. The method of claim 11 wherein said set of at least one second parameter includes an adjustable axis vector, an adjustable axis issue point and an adjustable cylinder radius which determine respectively

the orientation, position and size of said cylinder; said axis vector being adjustable from the initial radius line rotating around the center of the fitted sphere and with a predefined 3D angle variation; said axis issue point being adjustable along the neck axis in an interval between the center of the fitted sphere and the coordinate point on the neck axis of the orthogonal plane passing through the parallel of latitude α^*; the 3D correction boundary being fully determined from the quartet of parameters (α^*, axis vector, axis issue point, cylinder radius).

13. The method of claim 5 wherein the 3D boundary box is a cone constructed by the following steps:

i) determining a summit radial hemi-plane passing through the neck axis and said summit point of the 3D head-neck junction curve;
ii) determining a radius line of the fitted sphere passing at the intersection of said radial hemi-plane and the parallel of latitude α^*;
iii) positioning the cone so that its rotational axis is along said radius line and issued from the center of the fitted sphere;
iv) determining the aperture angle of the cone so that the intersection curve of the external wall of the cone with the 3D surface model extends to cover the clock interval and the summit point.

14. The method of claim 13 wherein said set of at least one second parameter includes an adjustable axis vector, an adjustable axis issue point and an adjustable aperture angle which determine respectively the orientation, position and aperture of the cone; said axis vector being adjustable from the initial radius line rotating around the center of the fitted sphere and with a predefined 3D angle variation; said axis issue point being adjustable along the neck axis in an interval between the center of the fitted sphere and the coordinate point on the neck axis of the orthogonal plane passing through the parallel of latitude α^*; the 3D correction boundary being fully determined from the quartet of parameters (α^*, axis vector, axis issue point, aperture angle).

15. The methods of any of claims 1 to 14, wherein the determination of the 3D spherical corrected surface patch and the 3D smooth transition corrected surface patch within the 3D correction boundary comprises the steps of:

i) splitting the 3D correction boundary in two contiguous regions by the parallel of latitude α^*, one distal region on the neck side and one proximal region on the head side, a portion of the parallel of latitude α^* forming a common boundary between said two contiguous regions;
ii) determining the 3D spherical corrected surface patch inside the proximal region as a pure spherical portion of the fitted sphere;
iii) determining the 3D smooth transition corrected surface patch inside the distal region by a 3D transition surface spline, said 3D transition surface spline being continuous with the 3D spherical corrected surface patch inside the proximal region along the common boundary, and continuous with the 3D bone surface model along its other boundary;

the union of the 3D spherical corrected surface patch and the 3D smooth transition corrected surface patch constituting a 3D corrected surface inside the 3D correction boundary.

16. The method of claim 15 wherein the surface tangents of said 3D transition surface spline are continuous with the surface tangents of the 3D spherical corrected surface patch along the common boundary, and the surface tangents of said 3D transition surface spline are continuous with the surface tangents of the 3D bone surface model along its other boundary.

17. The method of claim 16 wherein the 3D spherical corrected surface patch is further determined by a 3D spherical surface spline, said 3D spherical surface spline being continuous with the 3D smooth transition corrected surface patch along the common boundary and continuous with the 3D bone surface model along its other boundary, and wherein the surface tangents of the 3D spherical corrected surface patch are the tangents of the fitted sphere along the common boundary and the surface tangents of the 3D spherical corrected surface patch are continuous with the tangents of the 3D bone surface model along its other boundary.

18. The method according to any of claims 15 to 17 wherein the boundary of the distal region is composed of the two following portions:

i) the common boundary, and
ii) an external distal boundary being the boundary of the distal region minus the common boundary;

and wherein the 3D transition surface spline is constructed from surface interpolation between a set of radial 3D Bezier curves of degree at least 3, located at regular clock intervals on the clock correction interval.

19. The method of claim 18 wherein each of the radial 3D Bezier curve is determined by a distal extremity control point located on the 3D bone surface model along the external distal boundary, and a proximal

extremity control point located on the fitted sphere along the common boundary.

20. The method of claim 19 wherein each of the radial 3D Bezier curve slope is determined by a distal slope control point located on the 3D bone surface model, shifted proximally by a predetermined coefficient in the direction of the neck axis from the distal extremity control point, and by a proximal slope control point located at the end point of the radial vector of the corresponding radial index.

Patentansprüche

1. Verfahren zur nicht invasiven, reproduzierbaren Bestimmung einer korrigierten Oberfläche auf einem 3D-Knochenoberflächen-Modell, das aus einem medizinischen 3D-Bild eines Knochens mit einer Verformung konstruiert ist; wobei der Knochen einen an einem Halsabschnitt anliegenden Kopfabschnitt umfasst und die Knochenverformung aus einer Protuberanz-Hypertrophie an der Kopf-Halsnahtstelle besteht, wobei das genannte Verfahren das Bestimmen geometrischer Elemente, die die Anatomie des Knochens kennzeichnen, ausgehend von dem genannten 3D-Knochenoberflächen-Modell besteht, wobei die genannten geometrischen Elemente eine Kugel, die auf den sphärischen Abschnitt des Kopfes eingepasst ist, und eine Halsachse einschließen, wobei die genannte korrigierte Oberfläche **dadurch gekennzeichnet ist, dass** sie umfasst:

i) einen sphärischen korrigierten 3D-Oberflächen-Patch auf dem Kopfabschnitt des genannten 3D-Knochenoberflächen-Modells und
ii) einen korrigierten Oberflächen-Patch mit nahtlosem 3D-Übergang auf dem Halsabschnitt des genannten 3D-Knochenoberflächen-Modells, das an dem genannten sphärischen, korrigierten 3D-Oberflächen-Patch anliegend ist,

und wobei die genannten korrigierten Oberflächen-Patche durch einen Parametersatz definiert sind, umfassend:

iii) wenigstens einen ersten Parameter (α*), der einen sphärischen Ausdehnungswert des genannten sphärischen korrigierten 3D-Oberflächen-Patchs darstellt, wobei der genannte erste Parameter (α*) ein Zielwinkel ist, von dem erwartet wird, dass er nach dem operativen Eingriff erreicht ist, der radial zwischen der Halblinie, die aus dem Zentrum der eingepassten Kugel hervortritt und distal entlang der Halsachse ausgerichtet ist, und einem Radius der eingepassten Kugel gemessen ist
iv) und einen Satz von wenigstens einem zweiten Parameter zusätzlich zu dem genannten ersten Parameter, wobei der genannte Satz die 3D-Korrekturgrenze der genannten korrigierten Oberflächen-Patche bestimmt, wobei der wenigstens eine zweite Parameter das Ausmaß auf dem 3D-Knochenoberflächen-Modell der genannten 3D-Korrekturgrenze definiert,

derart, dass der genannte korrigierte Oberflächen-Patch mit nahtlosem 3D-Übergang entlang der genannten Grenze mit dem genannten 3D-Knochenoberflächen-Modell anliegend ist und derart, dass die Oberflächentangenten zu dem genannten korrigierten Oberflächen-Patch mit nahtlosem 3D-Übergang entlang der genannten Grenze mit den Oberflächentangenten des genannten 3D-Knochenoberflächen-Modells außerhalb der genannten Grenze anliegend sind.

2. Verfahren nach Anspruch 1, wobei der Parametersatz aus den genannten ersten und zweiten Parametern besteht.

3. Verfahren nach Anspruch 1 oder Anspruch 2, umfassend die folgenden Schritte:

i) Bestimmung eines Ziffernblatt-Bezugsystems auf dem Kopfabschnitt des um die Halsachse rotierenden Knochens ausgehend von dem genannten 3D-Knochenmodell und von den genannten geometrischen Elementen, die die Anatomie des Knochens charakterisieren;
ii) Bestimmung einer Kurve der 3D-Kopf-Halsnahtstelle auf dem 3D-Knochen-Oberflächenmodell, das die Kopf-Halsnahtstelle des Knochens um das Ziffernblatt-Bezugssystem kennzeichnet; und
iii) Bestimmung eines Scheitelpunktes, der das Maximum der Protuberanzverformung kennzeichnet, ausgehend von der Kurve der 3D-Kopf-Halsnahtstelle; wobei der genannte Scheitelpunkt der Punkt der genannten Kurve der 3D-Kopf-Halsnahtstelle ist, der dem Gipfelpunkt des sphärischen Abschnitts des Kopfes des Knochens am nächsten ist;

und wobei die 3D-Korrekturgrenze sich proximal bis zu dem genannten Scheitelpunkt erstreckt.

4. Verfahren nach Anspruch 3, umfassend weiterhin die folgenden Schritte:

i) Bestimmung der Parallele der Breite α* der eingepassten Kugel;
ii) Bestimmung von zwei radialen Halbebenen, die die Halsachse enthalten und jeweils am Schnittpunkt der genannten Parallele der Breite α* und der Kurve der 3D-Kopf-Halsnahtstelle

verlaufen; wobei die Uhrenindexe dieser zwei Halbebenen auf dem genannten Ziffernblatt-Bezugssystem ein Korrektur-Uhrenintervall bestimmen;

iii) Bestimmung einer um den genannten Scheitelpunkt der Kurve der 3D-Kopf-Halsnahtstelle geschlossenen Kontur auf dem 3D-Knochenoberflächen-Modell, wobei sich die Kontur wenigstens distal zur Parallele der Breite α^* erstreckt und wenigstens radial das Korrektur-Uhrintervall abdeckt, wobei die genannte geschlossene Kontur die 3D-Korrekturgrenze ist.

5. Verfahren nach Anspruch 4, wobei die geschlossene Kontur auf dem 3D-Knochenoberflächen-Modell, die die 3D-Korrekturgrenze definiert, aus dem Schnittpunkt des 3D-Knochenoberflächen-Modells mit einem 3D-Grenzkasten besteht, wobei der genannte 3D-Grenzkasten eine geometrische 3D-Konstruktion ist, die von wenigstens dem zweiten Parameter definiert ist.

6. Verfahren nach Anspruch 5, wobei der genannte 3D-Grenzkasten ein Vielflach ist.

7. Verfahren nach Anspruch 6, wobei das genannte Vielflach eine geometrische Konstruktion ist, die durch die folgenden vier Grenzen begrenzt ist:

i) eine proximale Grenze, die durch einen Abschnitt des Schnittpunktes des 3D-Knochenoberflächen-Modells mit einer flachen Orthogonalen zur Halsachse definiert ist und durch den Scheitelpunkt der Kurve der 3D-Kopf-Halsnahtstelle verläuft, die in dem Korrekturintervall eingeschlossen ist;

ii) zwei radiale Grenzen, die durch zwei Knochenkonturen jeweils durch die zwei Halbebenen, die das Korrektur-Uhrenintervall bestimmen, als die Schnittpunkte des 3D-Knochenoberflächen-Modells definiert sind;

iii) eine distale Grenze, die durch eine 3D-Halskurve definiert ist, die als der Schnittpunkt des 3D-Oberflächenmodells durch eine zur Halsachse orthogonale Ebene definiert ist; wobei die Koordinatenposition entlang der Halsachse einen distalen Punkt (N0) definiert, der der wenigstens zweite Parameter ist und der weiter unten in der Halsrichtung in einer Entfernung von wenigstens dem Radius der eingepassten Kugel von dem Zentrum der eingepassten Kugel angeordnet ist;

wobei die 3D-Korrekturgrenze vollumfänglich von dem Parameterpaar (α^*, distaler Punkt) bestimmt ist.

8. Verfahren nach Anspruch 6, wobei das genannte Vielflach eine geometrische Konstruktion ist, die durch die folgenden vier Grenzen begrenzt ist:

i) eine proximale Grenze, die durch einen Abschnitt des Schnittpunkts des 3D-Knochenoberflächen-Modells mit einer zur Halsachse orthogonalen Ebene, die durch den Scheitelpunkt der Kurve der 3D-Kopf-Halsnahtstelle hindurchtritt, die im Korrekturintervall eingeschlossen ist;

ii) zwei radiale Grenzen, die durch die zwei Knochenkonturen definiert sind, die jeweils durch die zwei Halbebenen, die das Korrektur-Uhrenintervall bestimmen, als der Schnittpunkt des 3D-Knochenoberflächen-Modells definiert sind;

iii) eine distale Grenze, die durch eine 3D-Halskurve definiert ist, die durch eine zur Halsachse orthogonale Ebene als der Schnittpunkt des 3D-Oberflächenmodells definiert ist; wobei die Koordinatenposition entlang der Halsachse einen distalen Punkt (N0) definiert, der der wenigstens zweite Parameter ist und der weiter unten in der Halsrichtung in einer Entfernung von wenigstens dem Radius der eingepassten Kugel von dem Zentrum der eingepassten Kugel ist; und :

wobei der genannte Satz aus wenigstens einem zweiten Parameter zwei anpassbare Uhrenindexe einschließt, die das Ausmaß des Korrektur-Uhrenintervalls steueren; wobei die zwei radialen Halbebenen, die diesen zwei Indexen entsprechen, neue Schnittpunkt-Konturen mit dem 3D-Oberflächenmodell produzieren, wobei die radialen Grenzen der 3D-Korrekturgrenze durch die genannten neuen Schnittpunkt-Konturen gebildet sind; wobei die 3D-Korrekturgrenze vollumfänglich von der Vierergruppe der Parameter (α^*, distaler Punkt, erster Uhrenindex, zweiter Uhrenindex) bestimmt ist.

9. Verfahren nach Anspruch 6, wobei das genannte Vielflach eine geometrische Konstruktion ist, die durch die folgenden vier Grenzen begrenzt ist:

i) eine proximale Grenze, die durch einen Abschnitt des Schnittpunkts des 3D-Knochenoberflächen-Modells mit einer zur Halsachse orthogonalen Ebene definiert ist und die durch den Scheitelpunkt der Kurve der 3D-Kopf-Halsnahtstelle hindurchtritt, die im Korrekturintervall eingeschlossen ist; wobei die Koordinatenposition der proximalen Grenze auf der Halsachse einen proximalen Punkt (N1) definiert;

ii) zwei radiale Grenzen, die durch die zwei Knochenkonturen definiert sind, die jeweils durch die zwei Halbebenen, die das Korrektur-Uhrenintervall bestimmen, als der Schnittpunkt des 3D-Knochenoberflächen-Modells definiert sind;

iii) eine distale Grenze, die durch eine 3D-Halskurve durch eine zur Halsachse orthogonale Ebene als der Schnittpunkt des 3D-Oberflä-

chenmodells definiert ist; wobei die Koordinatenposition entlang der Halsachse einen distalen Punkt (N0) definiert, der weiter unten in der Halsrichtung in einer Entfernung von wenigstens dem Radius der eingepassten Kugel vom Zentrum der eingepassten Kugel angeordnet ist, und:
wobei der genannte Satz aus wenigstens einem Parameter einen anpassbaren distalen Punkt auf der Halsachse einschließt, der eine distale anpassbare Ebene bestimmt, die orthogonal zur Halsachse ist und einen Schnittpunkt mit dem 3D-Oberflächenmodell auf dem distalen Abschnitt des Schenkelhalses bildet und somit eine neue distale Grenze produziert; wobei der anpassbare distale Punkt, der zwischen der Koordinate auf der Halsachse der Ebene, die durch die Parallele der Breite α^* hindurchtritt, und einer vordefinierten maximalen distalen Koordinate auf der Halsachse positioniert ist; wobei die 3D-Korrekturgrenze vollumfänglich von der Dreiergruppe der Parameter (α^*, proximaler Punkt, distaler Punkt) bestimmt ist.

10. Verfahren nach Anspruch 7 bis 9, wobei der genannte Satz aus wenigstens einem zweiten Parameter jeden Satz aus anpassbaren Parametern einschließt, die in den Ansprüchen 9 oder 10 definiert sind; wobei die genannte Kombination das Ausmaß der 3D-Korrekturgrenze kontrolliert; wobei die 3D-Korrekturgrenze vollumfänglich von dem Satz aus 5 Parametern bestimmt ist, die (α^*, proximaler Punkt, distaler Punkt, Uhrenindex 1, Uhrenindex 2) sind.

11. Verfahren nach Anspruch 5, wobei der 3D-Grenzkasten ein Zylinder ist, der durch die folgenden Schritte konstruiert ist:

i) Bestimmung eines radialen, halbebenen Scheitelpunktes, der durch die Halsachse und den genannten Scheitelpunkt der Kurve der 3D-Kopf-Halsnahtstelle hindurchtritt;
ii) Bestimmung einer Radiuslinie der eingepassten Kugel, die am Schnittpunkt des genannten radialen halbebenen Scheitelpunkts und der Parallele der Breite α^* hindurchtritt;
iii) Positionierung des Zylinders, so dass seine lange Achse entlang der definierten Radiuslinie verläuft;
iv) Bestimmung des Durchmessers des Zylinders, so dass die Schnittpunktkurve der Außenwand des Zylinders mit dem 3D-Oberflächenmodell sich erstreckt, um das Uhrenintervall und den Scheitelpunkt abzudecken.

12. Verfahren nach Anspruch 11, wobei der genannte Satz aus wenigstens einem zweiten Parameter einen anpassbaren Achsenvektor, einen anpassbaren Achsen-Ausgangspunkt und einen anpassbaren Zylinderradius einschließt, der jeweils die Ausrichtung, Position und Größe des genannten Zylinders bestimmt; wobei der genannte Achsenvektor von dem Anfangsradius einstellbar ist, der sich um das Zentrum der eingepassten Kugel und mit einer vordefinierten 3D-Winkelvariation dreht; wobei der genannte Achsenausgangspunkt entlang der Halsachse in einem Intervall zwischen dem Zentrum der eingepassten Kugel und dem Koordinatenpunkt auf der Halsachse der orthogonalen Ebene, die durch die Parallele der Breite α^* anpassbar ist anpassbar ist; wobei die 3D-Korrekturgrenze vollumfänglich von der Vierergruppe der Parameter (α^*, Achsenvektor, Achsenausgangspunkt, Zylinderradius) bestimmt ist.

13. Verfahren nach Anspruch 5, wobei der 3D-Grenzkasten ein Konus ist, der durch die folgenden Schritte konstruiert ist:

i) Bestimmung eines radialen Halbebenen-Scheitelpunktes, der durch die Halsachse und den genannten Scheitelpunkt der Kurve der 3D-Kopf-Halsnahtstelle hindurchtritt;
ii) Bestimmung einer Radiuslinie der eingepassten Kugel, die am Schnittpunkt der genannten radialen Halbebene und der Parallele der Breite α^* verläuft;
iii) Positionierung des Konus, so dass seine Rotationsachse entlang der genannten Radiuslinie verläuft und in dem Zentrum der eingepassten Kugel ihren Ursprung nimmt; und
iv) Bestimmung des Öffnungswinkels des Konus, so dass die Schnittpunktkurve der Außenwand des Konus sich mit dem 3D-Oberflächenmodell erstreckt, um das Uhrenintervall und den Scheitelpunkt abzudecken.

14. Verfahren nach Anspruch 13, wobei der genannte Satz aus wenigstens einem zweiten Parameter einen anpassbaren Achsenvektor, einen anpassbaren Achsenausgangspunkt und einen anpassbaren Öffnungswinkel einschließt, der jeweils die Ausrichtung, Position und Öffnung des Konus bestimmt; wobei der genannte Achsenvektor von der anfänglichen Radiuslinie, die sich um das Zentrum der eingepassten Kugel dreht, und mit einer vordefinierten 3D-Winkelvariation anpassbar ist; wobei der genannte Achsenausgangspunkt entlang der Halsachse in einem Intervall zwischen dem Zentrum der eingepassten Kugel und dem Koordinatenpunkt auf der Halsachse der orthogonalen Ebene die durch die Parallele der Breite α^* hindurchtritt, anpassbar ist; wobei die 3D-Korrekturgrenze vollumfänglich aus der Vierergruppe der Parameter (α^*, Achsenvektor, Achsenausgangspunkt, Öffnungswinkel) bestimmt ist.

15. Verfahren nach irgendeinem der Ansprüche 1 bis 14, wobei die Bestimmung des sphärischen, korrigierten 3D-Oberflächen-Patchs und dem korrigierten Oberflächen-Patch mit nahtlosem 3D-Übergang innerhalb der 3D-Korrekturgrenzen die Schritte umfasst:

i) Aufteilung der 3D-Korrekturgrenze in zwei anliegende Regionen durch die Parallele der Breite α*, eine distale Region auf der Halsseite und eine proximale Region auf der Kopfseite, wobei ein Abschnitt der Parallelen der Breite α* eine gemeinsame Grenze zwischen zwei anliegenden Regionen bildet;
ii) Bestimmung des sphärischen korrigierten 3D-Oberflächen-Patchs innerhalb der proximalen Region als einen reinen sphärischen Abschnitt der eingepassten Kugel; und
iii) Bestimmung des korrigierten Oberflächen-Patchs mit nahtlosem 3D-Übergang innerhalb der distalen Region durch einen 3D-Übergangsoberflächen-Spline, wobei der genannte 3D-Übergangsoberflächen-Spline mit dem sphärischen, korrigierten 3D-Oberflächen-Patch innerhalb der proximalen Region entlang der gemeinsamen Grenze und mit dem 3D-Knochenoberflächen-Modell entlang seiner anderen Grenze anliegend ist;

wobei die Verbindung des sphärischen, korrigierten 3D-Oberflächen-Patchs und dem korrigierten Oberflächen-Patch mit nahtlosem 3D-Übergang eine korrigierte 3D-Oberfläche innerhalb der 3D-Korrekturgrenze bilden.

16. Verfahren nach Anspruch 15, wobei die Oberflächen-Tangente des genannten 3D-Übergangsoberflächen-Splines mit den OberflächenTangenten des sphärischen, korrigierten 3D-Oberflächen-Patchs entlang der gemeinsamen Grenze kontinuierlich sind und die Oberflächentangenten des genannten 3D-Übergangsoberflächen-Splines mit den Oberflächentangenten des 3D-Knochenoberflächen-Modells entlang ihrer anderen Grenze kontinuierlich sind.

17. Verfahren nach Anspruch 16, wobei der sphärische, korrigierte 3D-Oberflächen-Patch weiterhin durch einen sphärischen 3D-Oberflächen-Spline bestimmt ist, wobei der genannte sphärische 3D-Oberflächen-Spline mit dem korrigierten Oberflächen-Patch mit nahtlosem 3D-Übergang entlang der gemeinsamen Grenze kontinuierlich ist und mit dem 3D-Knochenoberflächen-Modell entlang seiner anderen Grenze kontinuierlich ist und wobei die Oberflächentangenten des sphärischen, korrigierten 3D-Oberflächen-Patchs die Tangenten der eingepassten Kugel entlang der gemeinsamen Grenze sind und die Oberflächentangenten des sphärischen, korrigierten 3D-Oberflächen-Patchs mit den Tangenten des 3D-Knochenoberflächen-Modells entlang seiner anderen Grenze kontinuierlich sind.

18. Verfahren nach irgendeinem der Ansprüche 15 bis 17, wobei die Grenze der distalen Region aus den folgenden zwei Abschnitten zusammengesetzt ist:

i) der gemeinsamen Grenze und
ii) einer externen distalen Grenze, die die Grenze der distalen Region abzüglich der gemeinsamen Grenze ist;

und wobei der 3D-Übergangsoberflächen-Spline aus einer Oberflächen-Interpolation zwischen einem Satz aus radialen 3D-Bezierkurven wenigstens des Grades 3 konstruiert ist, die in regelmäßigen Uhrenintervallen auf dem Uhrenkorrektur-Intervall angeordnet sind.

19. Verfahren nach Anspruch 18, wobei jeder der radialen 3D-Bezierkurven durch einen distalen End-Kontrollpunkt bestimmt ist, der an dem 3D-Knochenoberflächen-Modell entlang der externen distalen Grenze und einem proximalen End-Kontrollpunkt, der auf der eingepassten Kugel entlang der gemeinsamen Grenze eingepasst ist, angeordnet ist.

20. Verfahren nach Anspruch 19, wobei die Neigung jeder radialen 3D-Bezierkurve durch einen distalen Neigungs-Kontrollpunkt bestimmt ist, der auf dem 3D-Knochenoberflächen-Modell angeordnet ist, proximal um einen vorbestimmten Koeffizienten in der Richtung der Halsachse von dem distalen End-kontroll-Punkt und um einen proximalen Neigungskontroll-Punkt versetzt ist, der am Endpunkt des radialen Vektors des entsprechenden radialen Indexes angeordnet ist.

Revendications

1. Procédé pour une détermination reproductible non invasive d'une surface corrigée sur un modèle de surface d'os 3D qui est construit à partir d'une image médicale 3D d'un os qui présente une déformation ; l'os comprenant une partie de tête qui est contiguë à une partie de col, et la déformation de l'os étant constituée par une hypertrophie en protubérance au niveau de la jonction tête-col, dans lequel ledit procédé comprend la détermination, à partir dudit modèle de surface d'os 3D, d'éléments géométriques qui caractérisent l'anatomie de l'os, lesdits éléments géométriques incluant une sphère qui est ajustée sur la partie sphérique de la tête et un axe du col ; dans lequel ladite surface corrigée est **caractérisée**

en ce qu'elle comprend :

i) un patch de surface corrigée sphérique 3D sur la partie de tête dudit modèle de surface d'os 3D ; et
ii) un patch de surface corrigée 3D de transition sans discontinuités sur la partie de col dudit modèle de surface d'os 3D, qui est contigu audit patch de surface corrigée sphérique 3D ;

et dans lequel lesdits patchs de surface corrigée sont définis par un jeu de paramètres qui comprennent :

iii) au moins un premier paramètre (α*) qui représente une valeur d'étendue sphérique dudit patch de surface corrigée sphérique 3D, ledit premier paramètre (α*) étant un angle cible, dont on s'attend à ce qu'il soit obtenu après chirurgie, qui est mesuré radialement entre la demi-ligne issue du centre de la sphère ajustée et orientée de façon distale le long de l'axe du col, et un rayon de la sphère ajustée ; et
iv) un jeu qui est constitué par au moins un second paramètre en plus dudit premier paramètre, ledit jeu déterminant la frontière de correction 3D desdits patchs de surface corrigée, ledit au moins un second paramètre définissant l'étendue sur le modèle de surface d'os 3D de ladite frontière de correction 3D,

de telle sorte que ledit patch de surface corrigée de transition sans discontinuités 3D soit continu avec ledit modèle de surface d'os 3D le long de ladite frontière de correction, et de telle sorte que les tangentes de surface par rapport audit patch de surface corrigée 3D de transition sans discontinuités le long de ladite frontière de correction soient continues avec les tangentes de surface dudit modèle de surface d'os 3D à l'extérieur de ladite frontière de correction.

2. Procédé selon la revendication 1, dans lequel le jeu de paramètres est constitué par lesdits premier et second paramètres.

3. Procédé selon la revendication 1 ou la revendication 2, comprenant en outre les étapes qui suivent :

i) la détermination, à partir dudit modèle de surface d'os 3D et à partir desdits éléments géométriques qui caractérisent l'anatomie de l'os, d'un référentiel de cadran d'horloge sur la partie de tête de l'os qui tourne autour de l'axe du col ;
ii) la détermination d'une courbe de jonction tête-col 3D sur le modèle de surface d'os 3D qui caractérise la jonction tête-col de l'os autour du référentiel de cadran d'horloge ; et
iii) la détermination, à partir de ladite courbe de jonction tête-col 3D, d'un point de sommet qui caractérise le maximum de la déformation en protubérance ; ledit point de sommet étant le point de ladite courbe de jonction tête-col 3D le plus proche du point d'apex de la partie sphérique de la tête de l'os ;

et dans lequel la frontière de correction 3D s'étend de façon proximale jusqu'audit point de sommet.

4. Procédé selon la revendication 3, comprenant en outre les étapes qui suivent :

i) la détermination du parallèle de latitude α* de la sphère ajustée ;
ii) la détermination de deux demi-plans radiaux qui contiennent l'axe du col et qui passent respectivement au niveau de l'intersection dudit parallèle de latitude α* et de la courbe de jonction tête-col 3D ; les index d'horloge de ces deux demi-plans sur ledit référentiel de cadran d'horloge déterminant un intervalle d'horloge de correction ; et
iii) la détermination, sur le modèle de surface d'os 3D, d'un contour fermé autour dudit point de sommet de la courbe de jonction tête-col 3D, lequel contour s'étend au moins de façon distale jusqu'au parallèle de latitude α*, et couvre au moins radialement l'intervalle d'horloge de correction, ledit contour fermé étant la frontière de correction 3D.

5. Procédé selon la revendication 4, dans lequel le contour fermé sur le modèle de surface d'os 3D qui définit la frontière de correction 3D est constitué par l'intersection du modèle de surface d'os 3D avec une boîte de frontière 3D, ladite boîte de frontière 3D étant une construction 3D géométrique qui est définie à partir d'au moins le second paramètre.

6. Procédé selon la revendication 5, dans lequel ladite boîte de frontière 3D est un polyèdre.

7. Procédé selon la revendication 6, dans lequel ledit polyèdre est une construction géométrique qui est délimitée par les quatre limites qui suivent :

i) une limite proximale qui est définie par une partie de l'intersection du modèle de surface d'os 3D avec un plan qui est orthogonal à l'axe du col et qui passe par le point de sommet de la courbe de jonction tête-col 3D qui est incluse dans l'intervalle d'horloge de correction ;
ii) deux limites radiales qui sont définies par les deux contours d'os qui sont respectivement définis en tant qu'intersection du modèle de surface d'os 3D par les deux demi-plans qui déterminent l'intervalle d'horloge de correction ;
iii) une limite distale qui est définie par une cour-

be de col 3D qui est définie en tant qu'intersection du modèle de surface d'os 3D par un plan qui est orthogonal à l'axe du col ; la position en termes de coordonnées le long de l'axe du col définissant un point distal (N0) qui est l'au moins un second paramètre et qui est localisé davantage vers le bas dans la direction du col à une distance d'au moins le rayon de la sphère ajustée par rapport au centre de la sphère ajustée ;

la frontière de correction 3D étant totalement déterminée à partir de l'ensemble des deux paramètres (α*, point distal).

8. Procédé selon la revendication 6, dans lequel ledit polyèdre est une construction géométrique qui est délimitée par les quatre limites qui suivent :

i) une limite proximale qui est définie par une partie de l'intersection du modèle de surface d'os 3D avec un plan qui est orthogonal à l'axe du col et qui passe par le point de sommet de la courbe de jonction tête-col 3D qui est incluse dans l'intervalle d'horloge de correction ;
ii) deux limites radiales qui sont définies par les deux contours d'os qui sont respectivement définis en tant qu'intersection du modèle de surface d'os 3D par les deux demi-plans qui déterminent l'intervalle d'horloge de correction ;
iii) une limite distale qui est définie par une courbe de col 3D qui est définie en tant qu'intersection du modèle de surface d'os 3D par un plan qui est orthogonal à l'axe du col ; la position en termes de coordonnées le long de l'axe du col définissant un point distal (N0) qui est l'au moins un second paramètre et qui est localisé davantage vers le bas dans la direction du col à une distance d'au moins le rayon de la sphère ajustée par rapport au centre de la sphère ajustée ;

et dans lequel ledit jeu qui est constitué par au moins un second paramètre inclut deux index d'horloge réglables qui commandent l'étendue de l'intervalle d'horloge de correction ; dans lequel les deux demi-plans radiaux qui correspondent à ces deux index produisent de nouveaux contours d'intersection avec le modèle de surface d'os 3D, les limites radiales de la frontière de correction 3D étant constituées par lesdits nouveaux contours d'intersection ; la frontière de correction 3D étant totalement déterminée à partir de l'ensemble des quatre paramètres (α*, point distal, premier index d'horloge, second index d'horloge).

9. Procédé selon la revendication 6, dans lequel ledit polyèdre est une construction géométrique qui est délimitée par les quatre limites qui suivent :

i) une limite proximale qui est définie par une partie de l'intersection du modèle de surface d'os 3D avec un plan qui est orthogonal à l'axe du col et qui passe par le point de sommet de la courbe de jonction tête-col 3D qui est incluse dans l'intervalle d'horloge de correction ; la position en termes de coordonnées de la limite proximale sur l'axe du col définissant un point proximal (N1) ;
ii) deux limites radiales qui sont définies par les deux contours d'os qui sont respectivement définis en tant qu'intersection du modèle de surface d'os 3D par les deux demi-plans qui déterminent l'intervalle d'horloge de correction ;
iii) une limite distale qui est définie par une courbe de col 3D qui est définie en tant qu'intersection du modèle de surface d'os 3D par un plan qui est orthogonal à l'axe du col ; la position en termes de coordonnées le long de l'axe du col définissant un point distal (N0) qui est localisé davantage vers le bas dans la direction du col à une distance d'au moins le rayon de la sphère ajustée par rapport au centre de la sphère ajustée ;

et dans lequel ledit jeu qui est constitué par au moins un second paramètre inclut un point distal réglable sur l'axe du col qui détermine un plan réglable distal qui est orthogonal à l'axe du col et qui intersecte le modèle de surface d'os 3D sur la partie distale du col fémoral, produisant ainsi une nouvelle limite distale ; le point distal réglable étant positionné entre la coordonnée sur l'axe du col du plan qui passe par le parallèle de latitude α* et une coordonnée distale maximum prédéfinie sur l'axe du col ; la frontière de correction 3D étant totalement déterminée à partir de l'ensemble des trois paramètres (α*, point proximal, point distal).

10. Procédé selon l'une quelconque des revendications 7 à 9, dans lequel ledit jeu qui est constitué par au moins un second paramètre inclut l'un quelconque des jeux de paramètres réglables qui sont définis selon les revendications 9 ou 10 ; laquelle combinaison commande l'étendue de la frontière de correction 3D ; la frontière de correction 3D étant totalement déterminée à partir de l'ensemble de cinq paramètres que sont (α*, point proximal, point distal, index d'horloge 1, index d'horloge 2).

11. Procédé selon la revendication 5, dans lequel la boîte de frontière 3D est un cylindre qui est construit au moyen des étapes qui suivent :

i) la détermination d'un demi-plan radial de sommet qui passe par l'axe du col et par ledit point de sommet de la courbe de jonction tête-col 3D ;
ii) la détermination d'une ligne de rayon de la

sphère ajustée qui passe au niveau de l'intersection dudit demi-plan radial de sommet et du parallèle de latitude α^* ;
iii) le positionnement du cylindre de telle sorte que son axe long soit le long de la ligne de rayon définie ; et
iv) la détermination du diamètre du cylindre de telle sorte que la courbe d'intersection de la paroi externe du cylindre avec le modèle de surface d'os 3D s'étende de manière à couvrir l'intervalle d'horloge de correction et le point de sommet.

12. Procédé selon la revendication 11, dans lequel ledit jeu qui est constitué par au moins un second paramètre inclut un vecteur d'axe réglable, un point d'origine d'axe réglable et un rayon de cylindre réglable qui déterminent respectivement l'orientation, la position et la taille dudit cylindre ; ledit vecteur d'axe pouvant être réglé à partir de la ligne de rayon initiale qui tourne autour du centre de la sphère ajustée et selon une variation d'angle 3D prédéfinie ; ledit point d'origine d'axe réglable pouvant être réglé le long de l'axe du col à l'intérieur d'un intervalle entre le centre de la sphère ajustée et le point de coordonnée sur l'axe du col du plan orthogonal qui passe par le parallèle de latitude α^* ; la frontière de correction 3D étant totalement déterminée à partir de l'ensemble des quatre paramètres (α^*, vecteur d'axe, point d'origine d'axe, rayon de cylindre).

13. Procédé selon la revendication 5, dans lequel la boîte de frontière 3D est un cône qui est construit au moyen des étapes qui suivent :

i) la détermination d'un demi-plan radial de sommet qui passe par l'axe du col et par ledit point de sommet de la courbe de jonction tête-col 3D ;
ii) la détermination d'une ligne de rayon de la sphère ajustée qui passe au niveau de l'intersection dudit demi-plan radial de sommet et du parallèle de latitude α^* ;
iii) le positionnement du cône de telle sorte que son axe de rotation soit le long de ladite ligne de rayon et parte du centre de la sphère ajustée ; et
iv) la détermination de l'angle d'ouverture du cône de telle sorte que la courbe d'intersection de la paroi externe du cône avec le modèle de surface d'os 3D s'étende de manière à ce qu'elle couvre l'intervalle d'horloge de correction et le point de sommet.

14. Procédé selon la revendication 13, dans lequel ledit jeu qui est constitué par au moins un second paramètre inclut un vecteur d'axe réglable, un point d'origine d'axe réglable et un angle d'ouverture réglable qui déterminent respectivement l'orientation, la position et l'ouverture du cône ; ledit vecteur d'axe pouvant être réglé par rapport à la ligne de rayon initiale autour du centre de la sphère ajustée et selon une variation d'angle 3D prédéfinie ; ledit point d'origine d'axe pouvant être réglé le long de l'axe du col à l'intérieur d'un intervalle entre le centre de la sphère ajustée et le point de coordonnée sur l'axe du col du plan orthogonal qui passe par le parallèle de latitude α^* ; la frontière de correction 3D étant totalement déterminée à partir de l'ensemble des quatre paramètres (α^*, vecteur d'axe, point d'origine d'axe, angle d'ouverture).

15. Procédé selon l'une quelconque des revendications 1 à 14, dans lequel la détermination du patch de surface corrigée sphérique 3D et du patch de surface corrigée 3D de transition sans discontinuités à l'intérieur de la frontière de correction 3D comprend les étapes de :

i) séparation de la frontière de correction 3D selon deux régions contiguës par le parallèle de latitude α^*, soit une région distale du côté du col et une région proximale du côté de la tête, une partie du parallèle de latitude α^* formant une frontière commune entre lesdites deux régions contiguës ;
ii) la détermination du patch de surface corrigée sphérique 3D à l'intérieur de la région proximale en tant que partie purement sphérique de la sphère ajustée; et
iii) la détermination du patch de surface corrigée 3D de transition sans discontinuités à l'intérieur de la région distale au moyen d'une fonction spline de surface de transition 3D, ladite fonction spline de surface de transition 3D étant continue avec le patch de surface corrigée sphérique 3D à l'intérieur de la région proximale le long de la frontière commune et étant continue avec le modèle de surface d'os 3D le long de son autre frontière ;

l'union du patch de surface corrigée sphérique 3D et du patch de surface corrigée de transition sans discontinuités 3D constituant une surface corrigée 3D à l'intérieur de la frontière de correction 3D.

16. Procédé selon la revendication 15, dans lequel les tangentes de surface de ladite fonction spline de surface de transition 3D sont continues avec les tangentes de surface du patch de surface corrigée sphérique 3D le long de la frontière commune, et les tangentes de surface de ladite fonction spline de surface de transition 3D sont continues avec les tangentes de surface du modèle de surface d'os 3D le long de son autre frontière.

17. Procédé selon la revendication 16, dans lequel le

patch de surface corrigée sphérique 3D est en outre déterminé au moyen d'une fonction spline de surface sphérique 3D, ladite fonction spline de surface sphérique 3D étant continue avec le patch de surface corrigée de transition sans discontinuités 3D le long de la frontière commune et étant continue avec le modèle de surface d'os 3D le long de son autre frontière, et dans lequel les tangentes de surface du patch de surface corrigée sphérique 3D sont les tangentes de la sphère ajustée le long de la frontière commune et les tangentes de surface du patch de surface corrigée sphérique 3D sont continues avec les tangentes du modèle de surface d'os 3D le long de son autre frontière.

18. Procédé selon l'une quelconque des revendications 15 à 17, dans lequel la frontière de la région distale est composée par les deux parties qui suivent :

i) la frontière commune ; et
ii) une frontière distale externe qui est la frontière de la région distale moins la frontière commune ;

et dans lequel la fonction spline de surface de transition 3D est construite à partir d'une interpolation de surface entre un jeu de courbes de Bézier 3D radiales d'un degré d'au moins 3, qui sont localisées selon des intervalles d'horloge réguliers sur l'intervalle d'horloge de correction.

19. Procédé selon la revendication 18, dans lequel chacune des courbes de Bézier 3D radiales est déterminée au moyen d'un point de commande d'extrémité distal qui est localisé sur le modèle de surface d'os 3D le long de la frontière distale externe, et au moyen d'un point de commande d'extrémité proximal qui est localisé sur la sphère ajustée le long de la frontière commune.

20. Procédé selon la revendication 19, dans lequel chacune des pentes des courbes de Bézier 3D radiales est déterminée au moyen d'un point de commande de pente distal qui est localisé sur le modèle de surface d'os 3D, décalé de façon proximale d'un coefficient prédéterminé dans la direction de l'axe du col par rapport au point de commande d'extrémité distal, et au moyen d'un point de commande de pente proximal qui est localisé au niveau du point d'extrémité du vecteur radial de l'index radial correspondant.

FIGURE 1

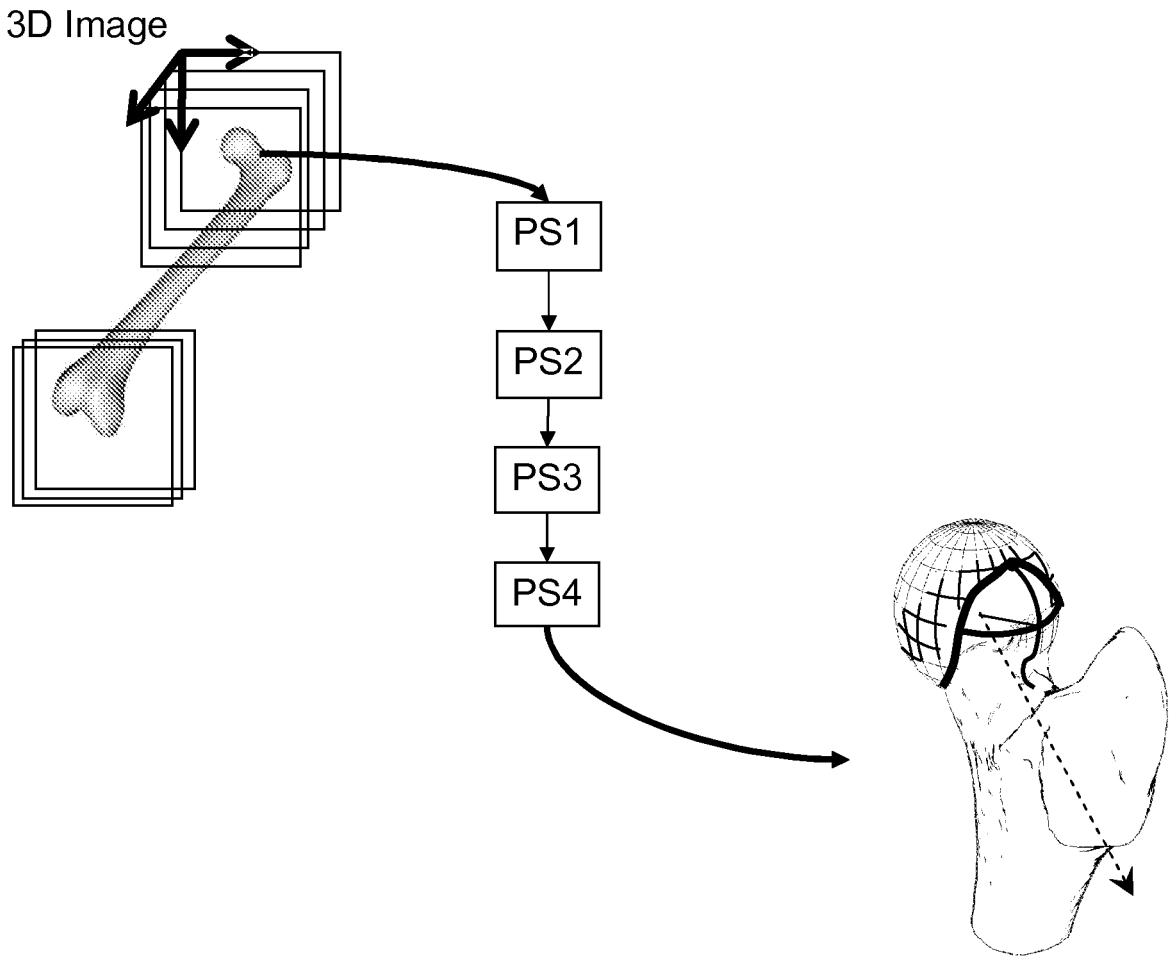

FIGURE 2A

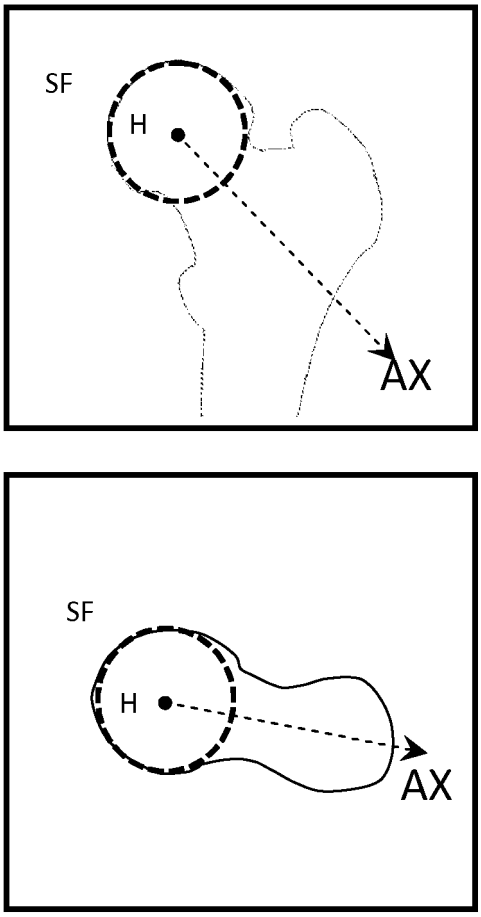

FIGURE 2B

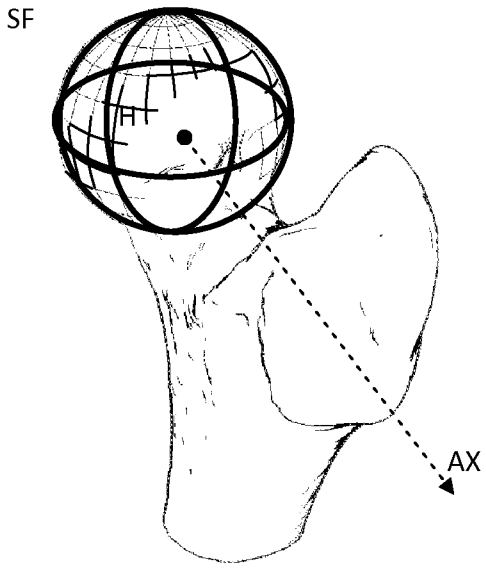

FIGURE 3

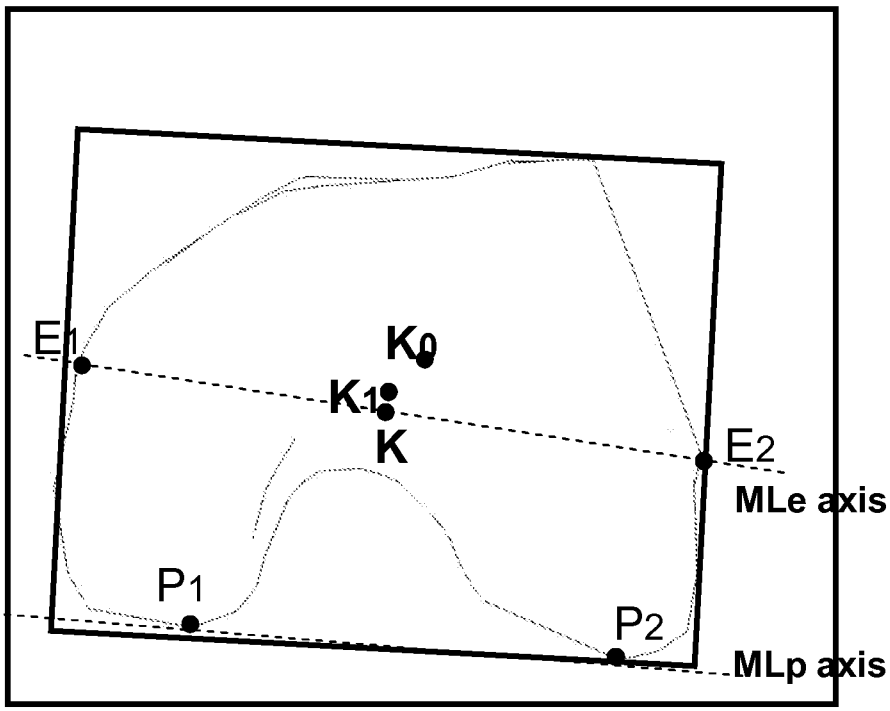

FIGURE 4A

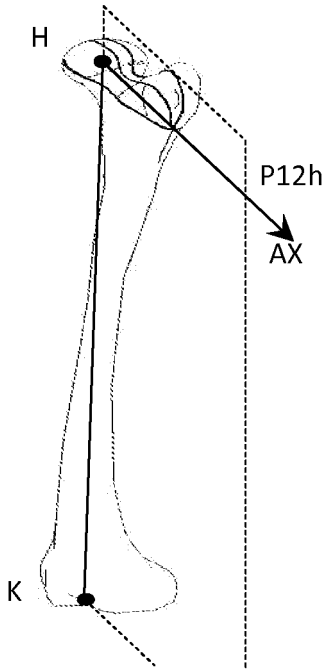

FIGURE 4B

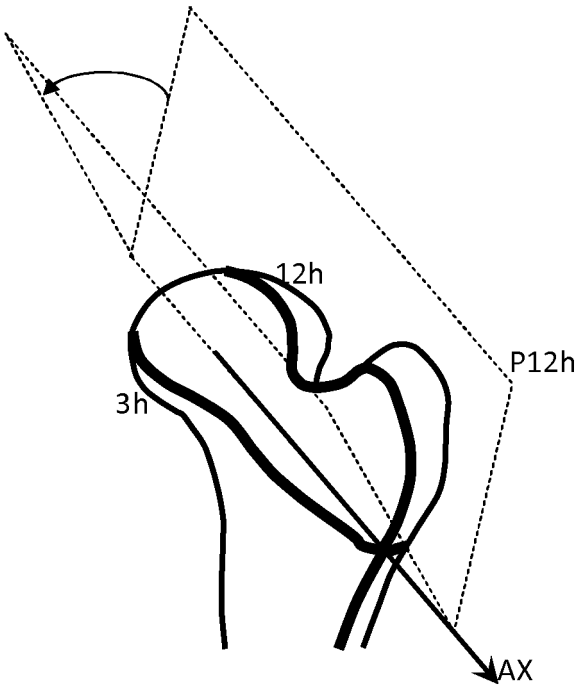

FIGURE 5

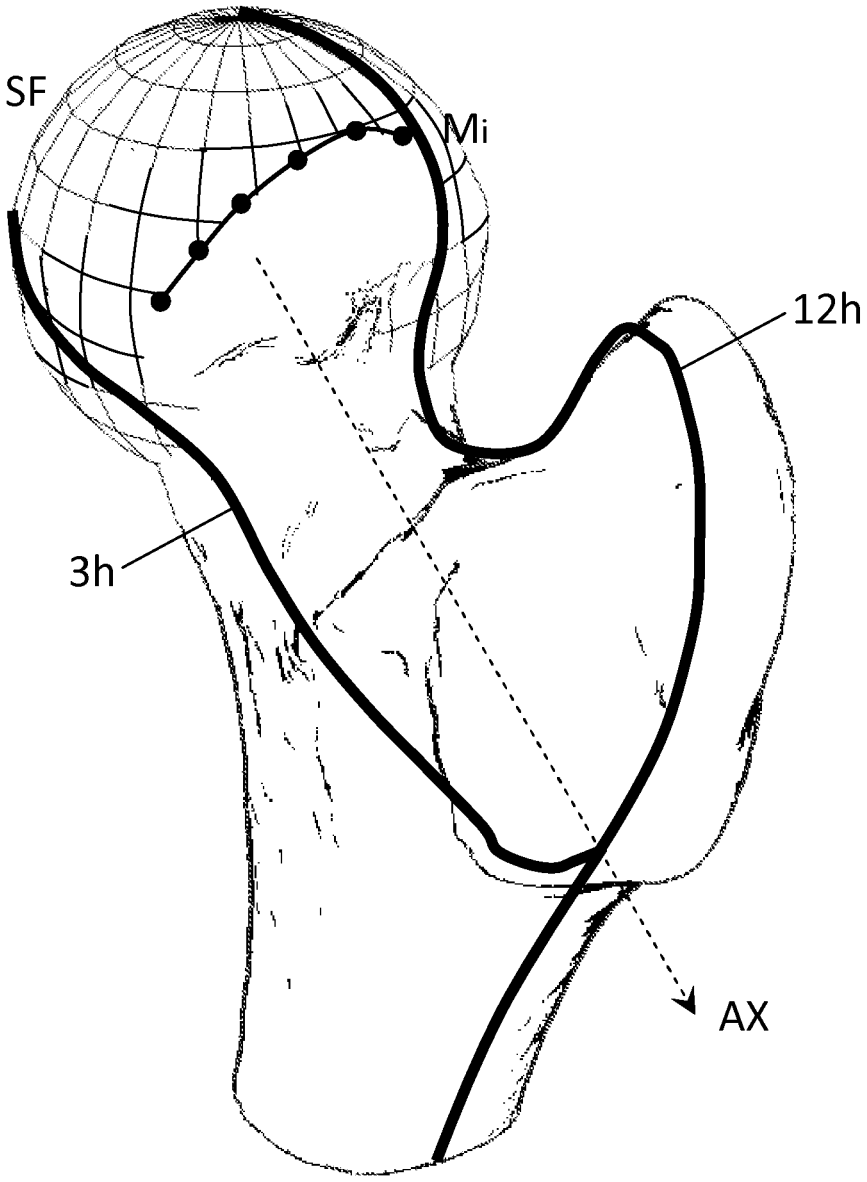

FIGURE 6

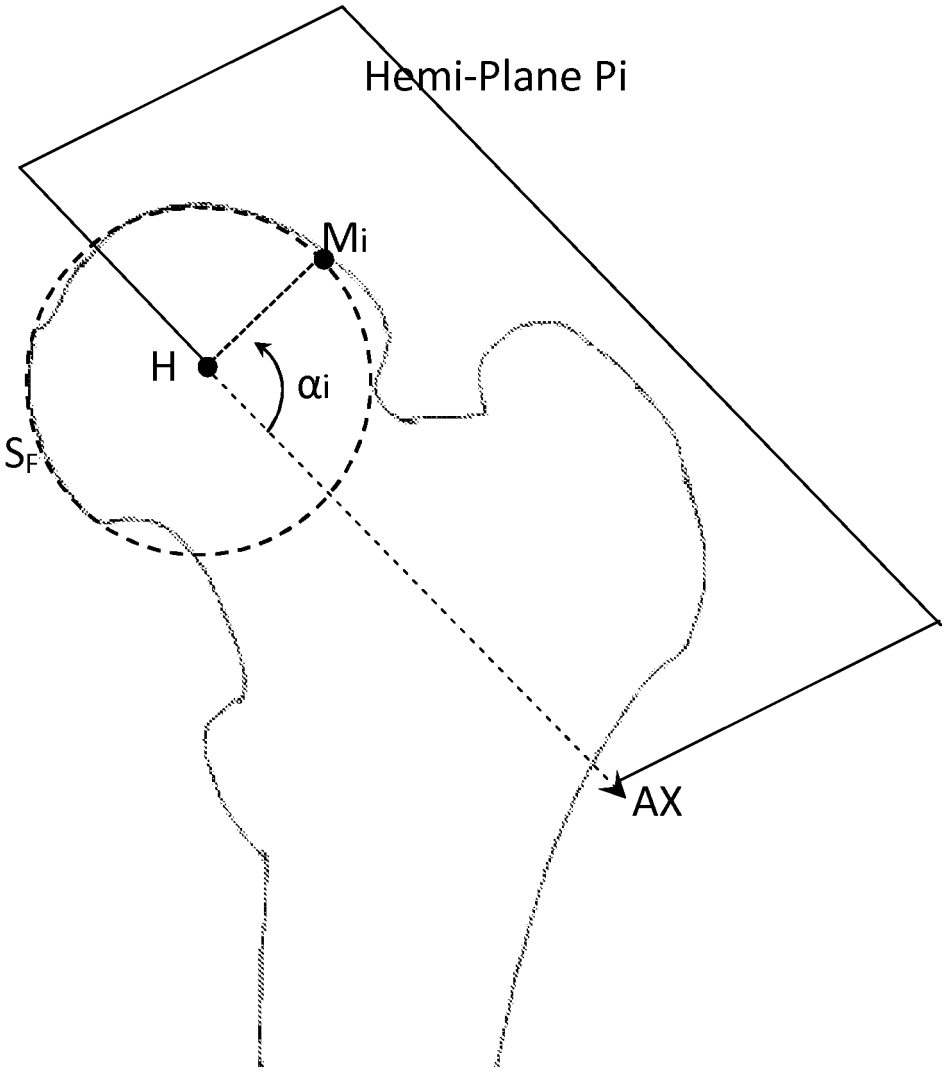

FIGURE 7

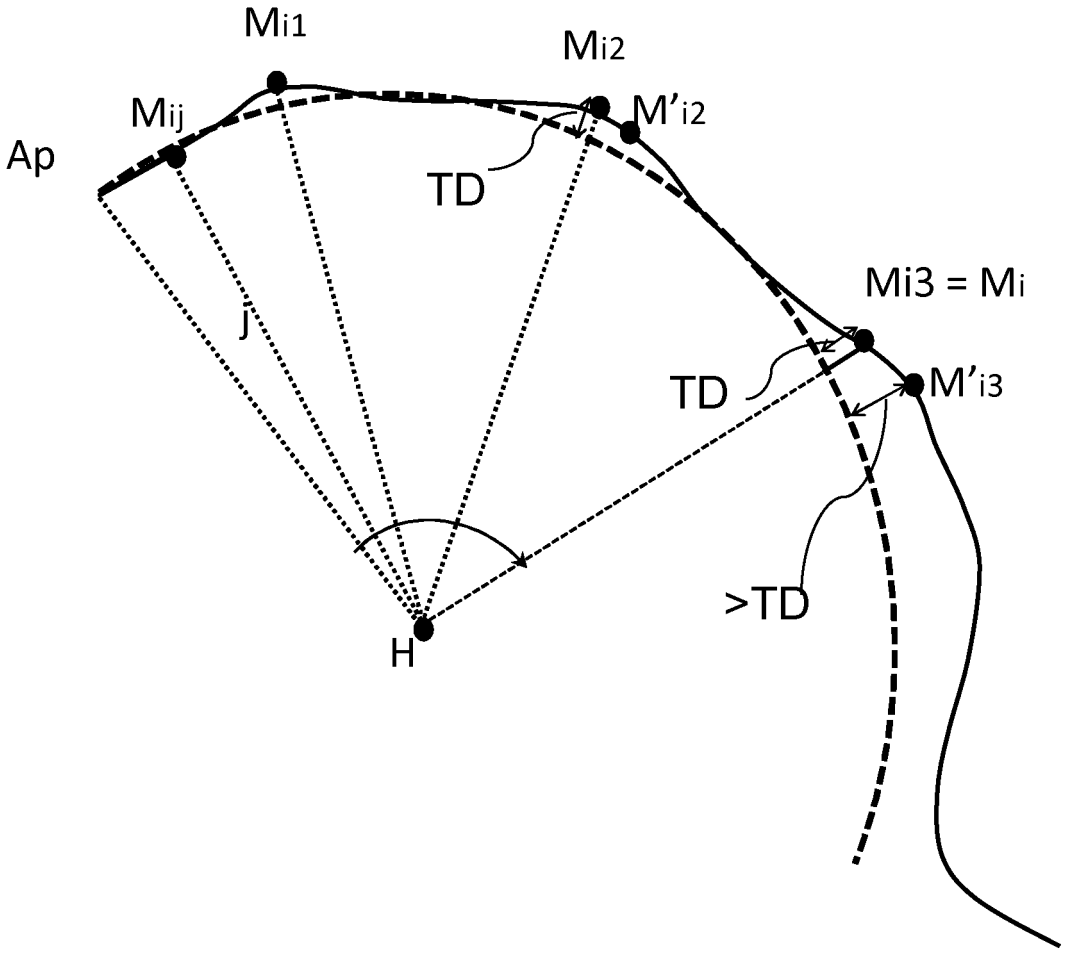

FIGURE 8

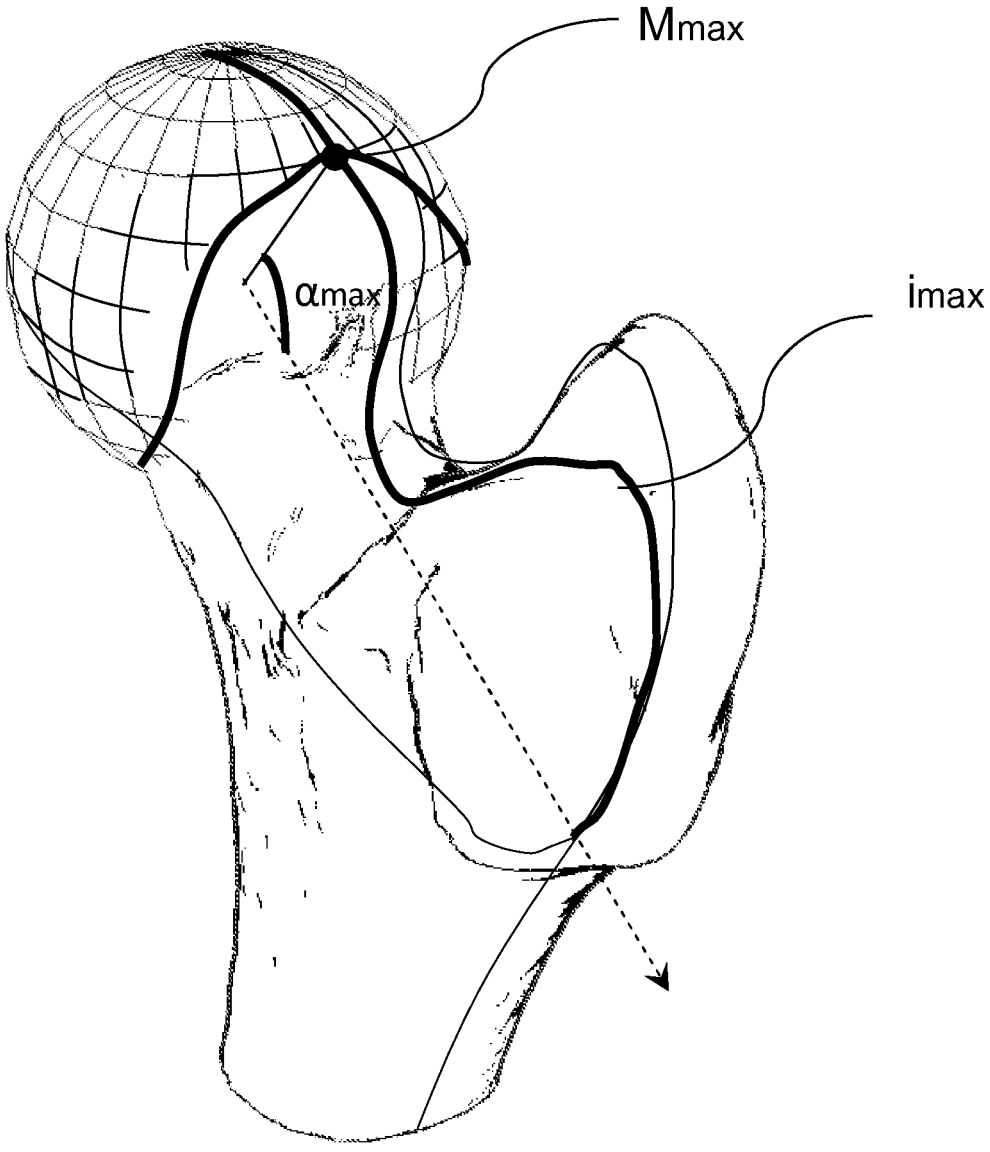

FIGURE 9A

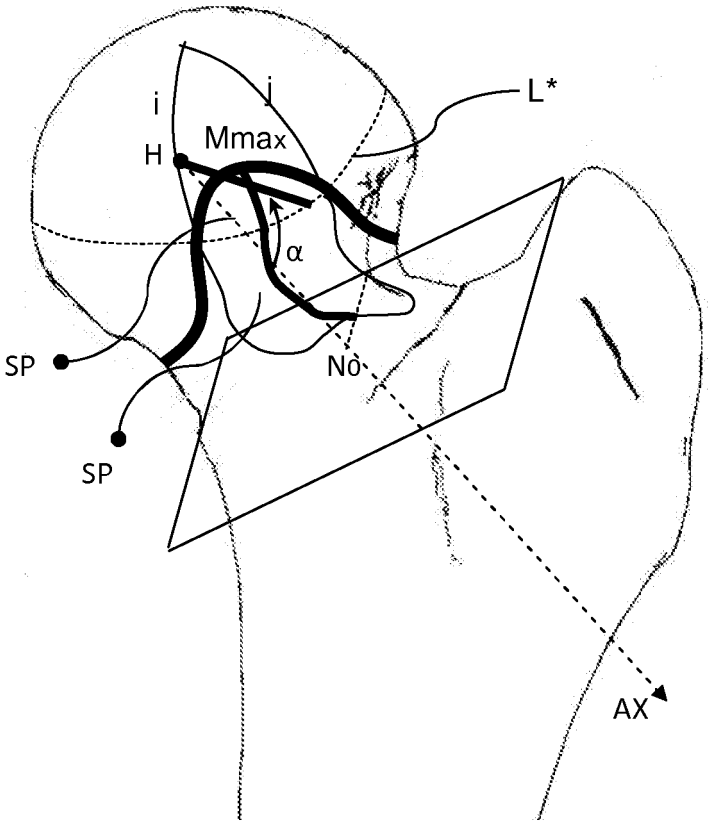

FIGURE 9B

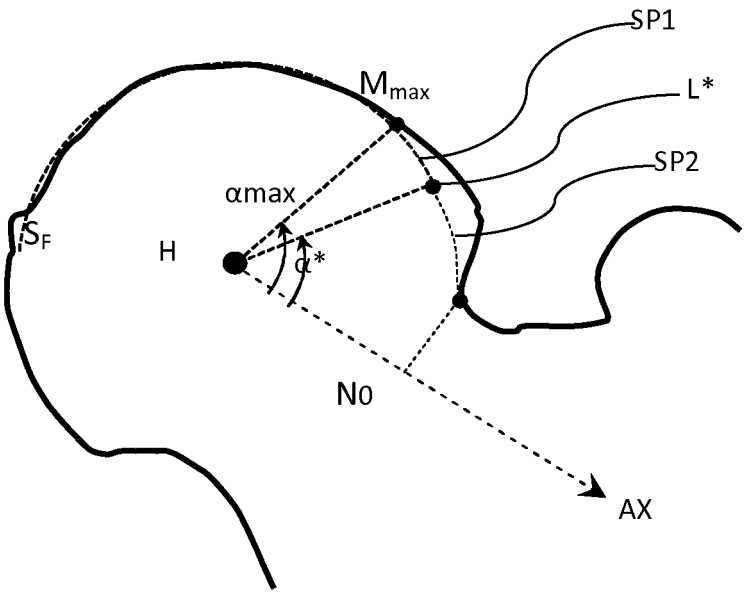

Hemi-Plane Pi_{Max}

FIGURE 10A

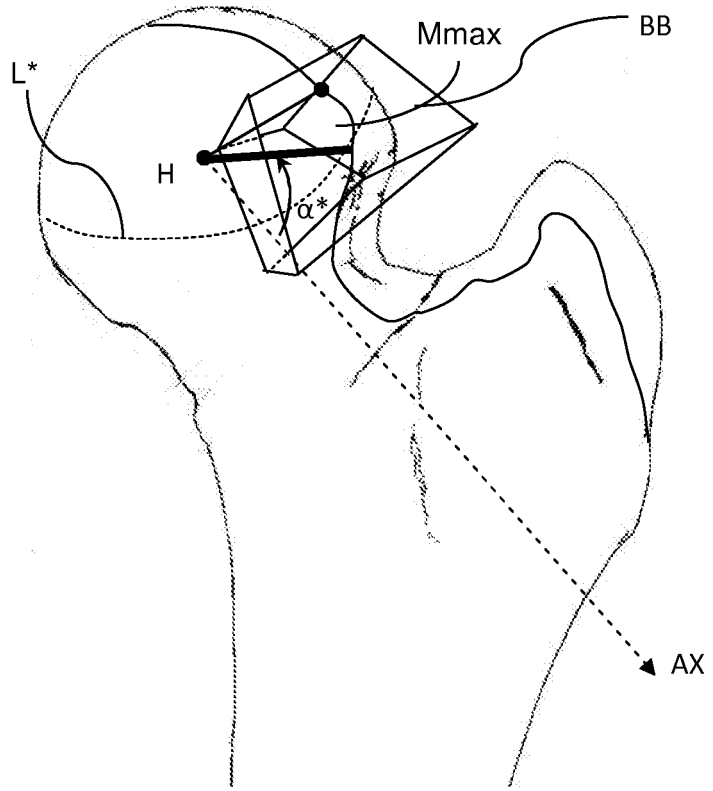

FIGURE 10B

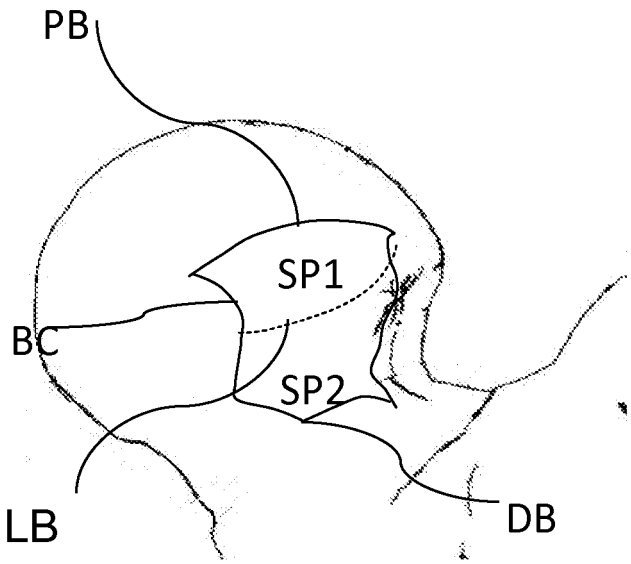

FIGURE 11

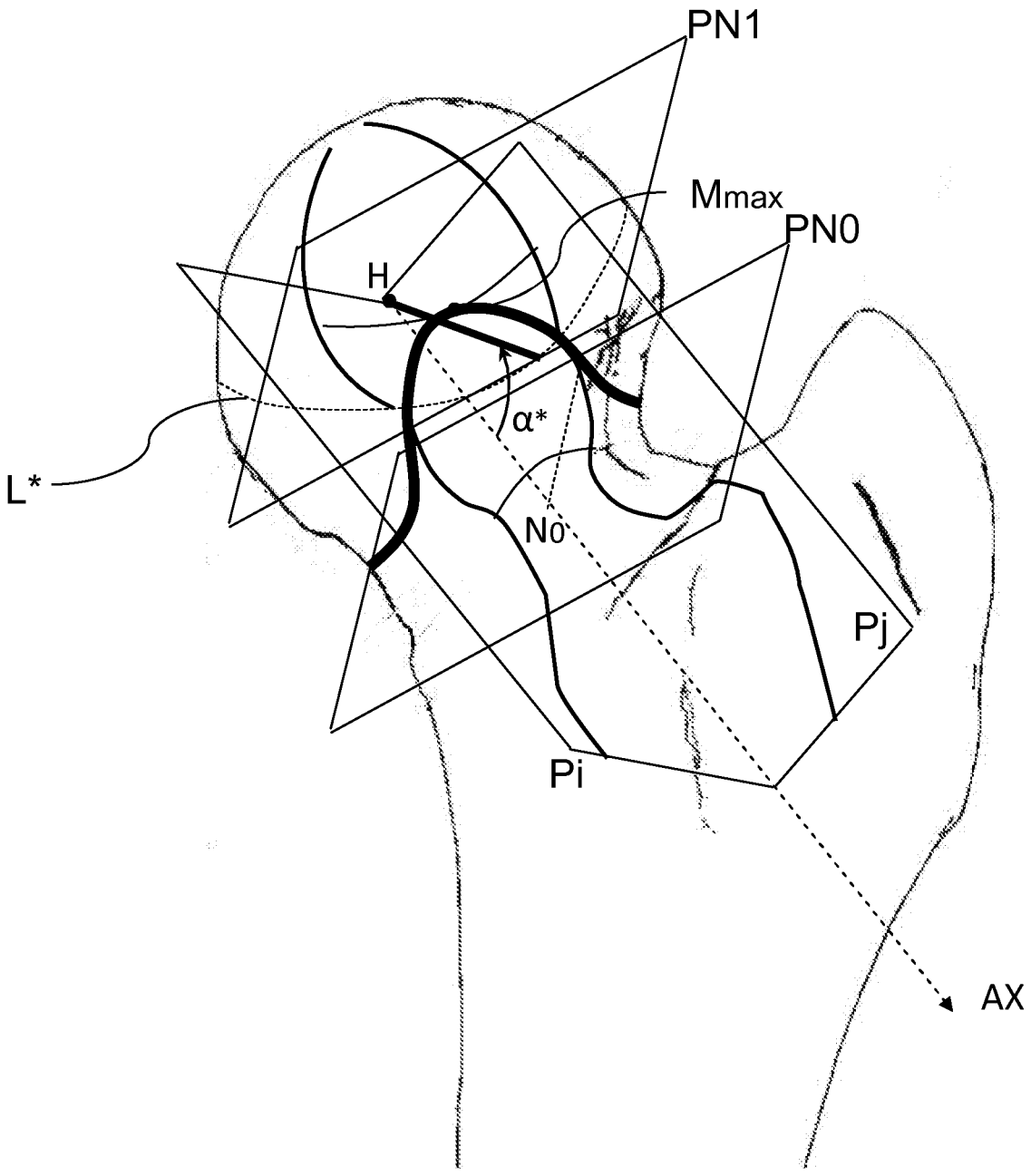

FIGURE 12

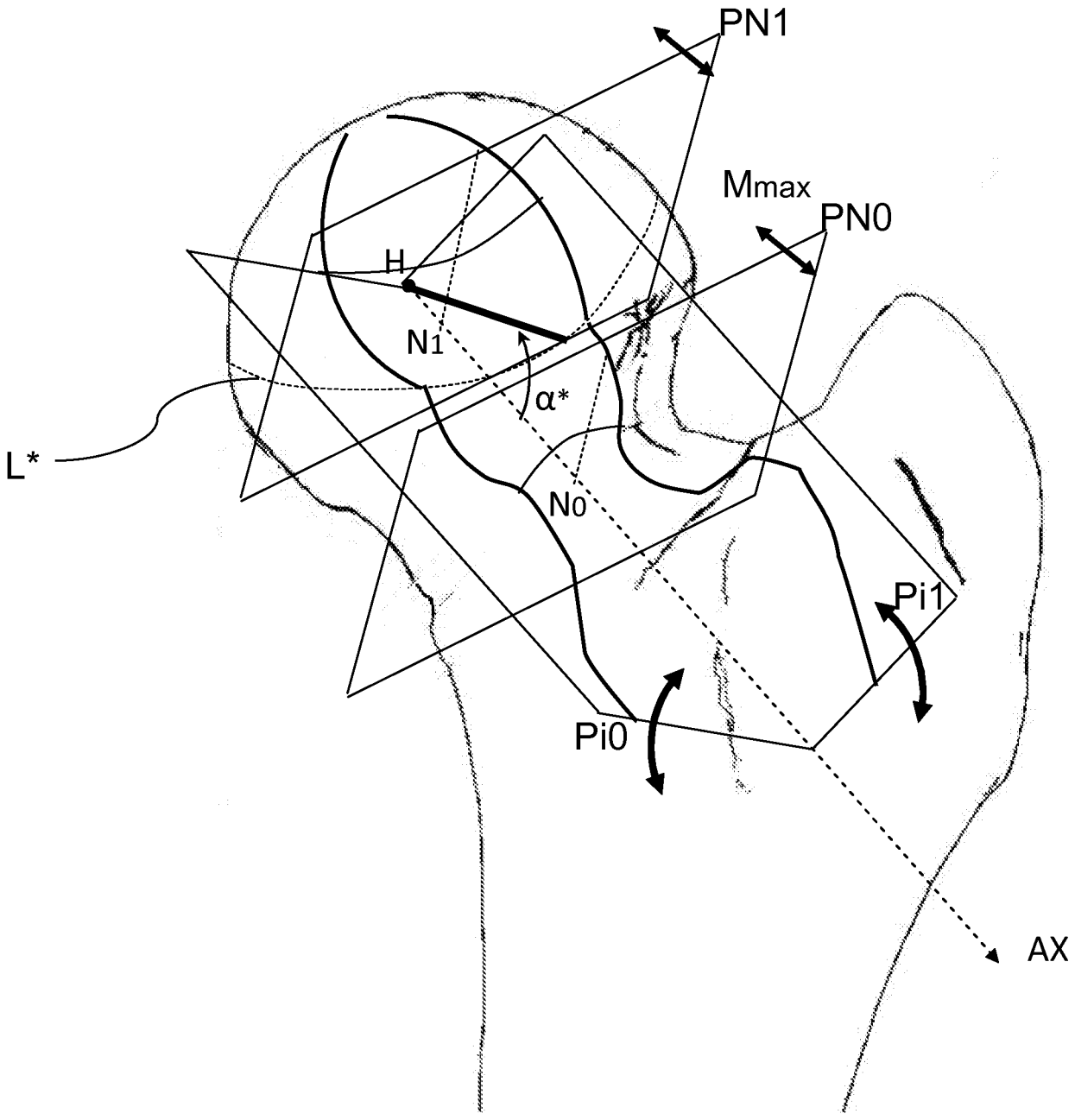

FIGURE 13A

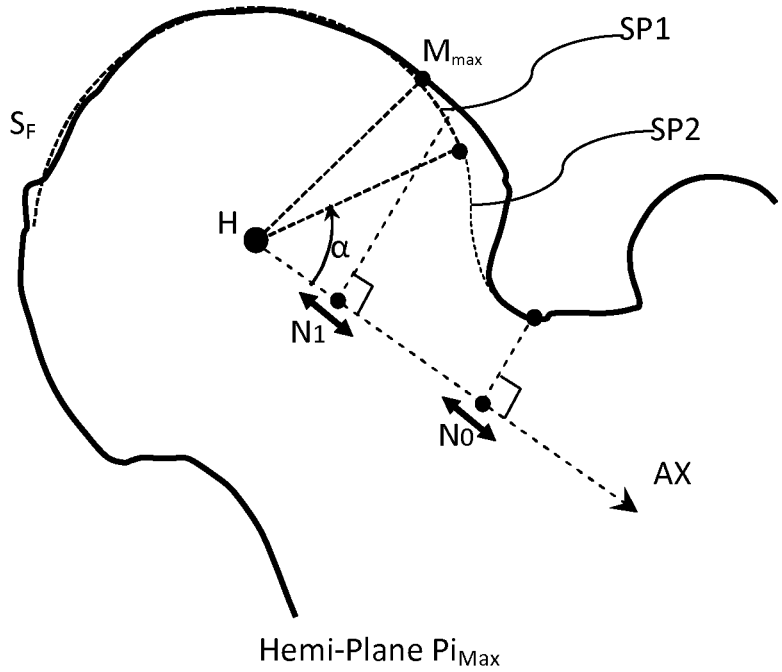

FIGURE 13B

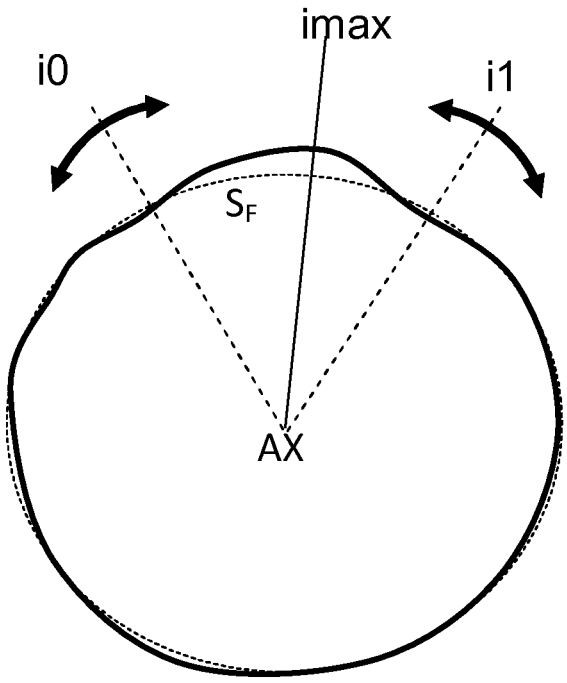

FIGURE 14

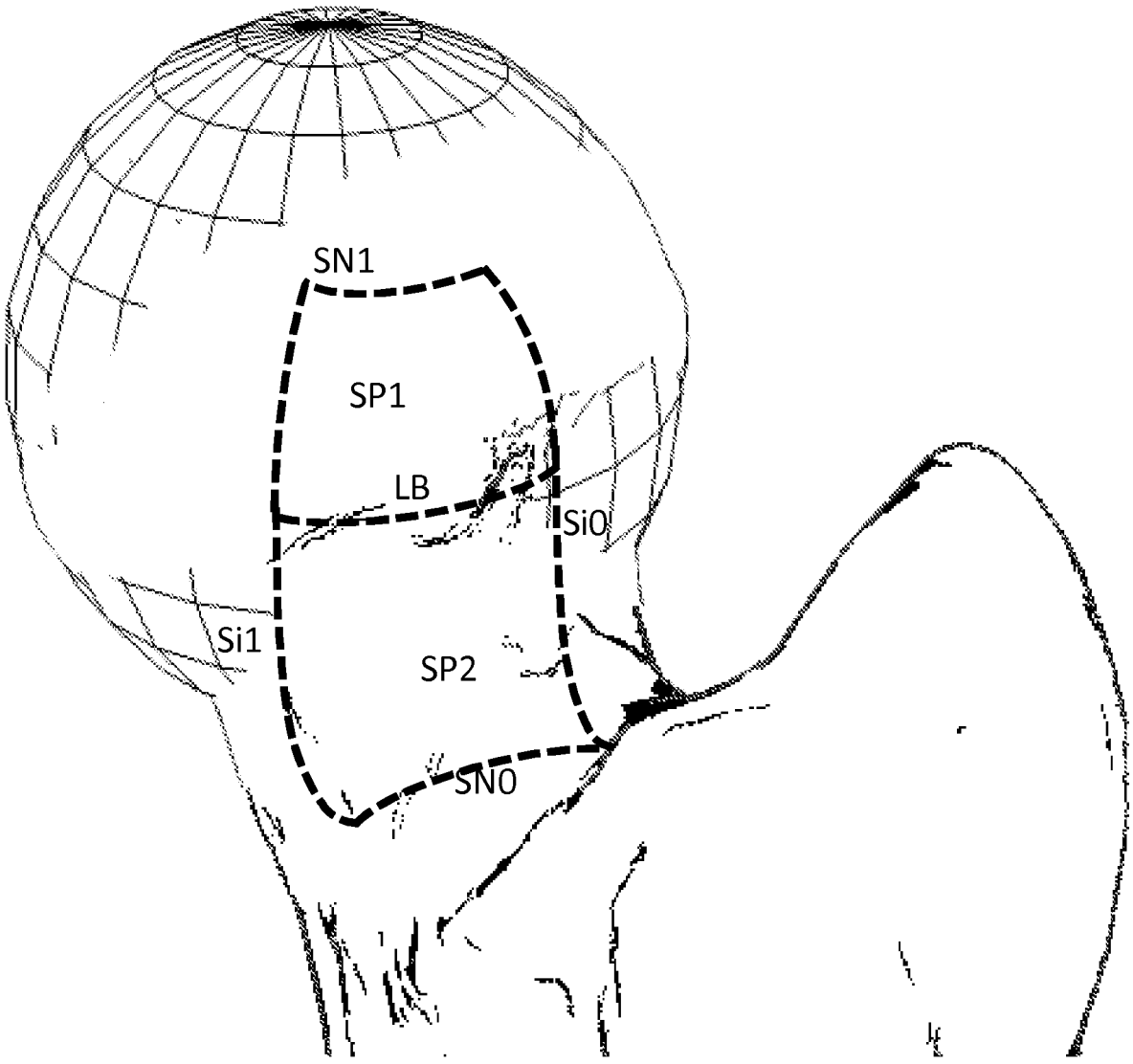

FIGURE 15A

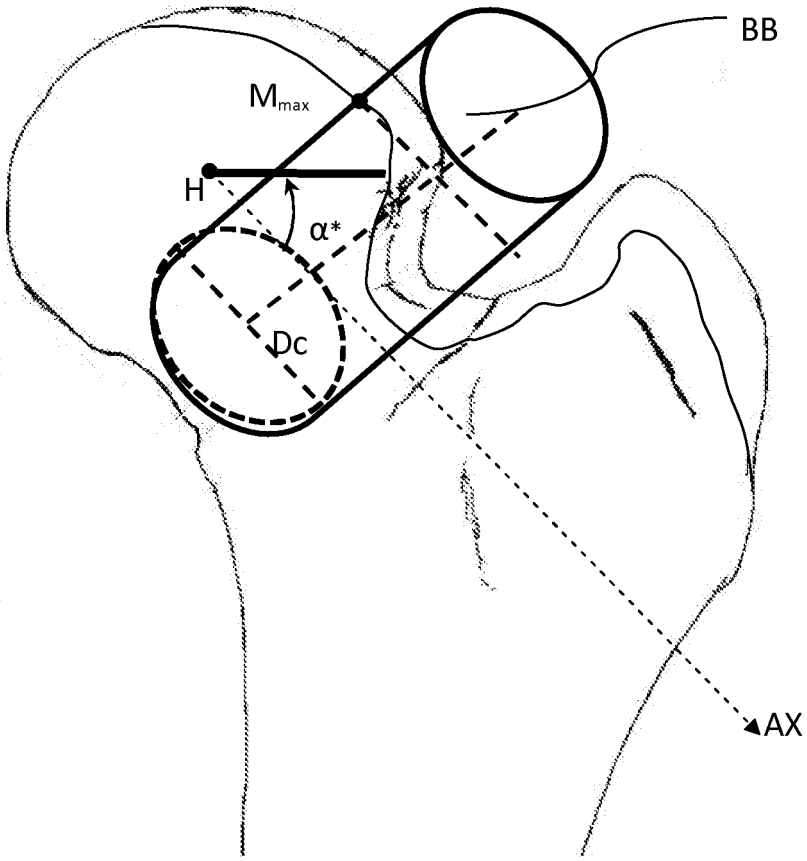

FIGURE 15B

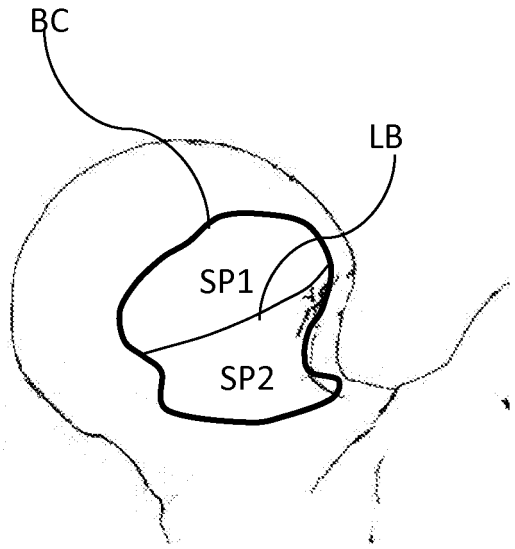

FIGURE 16A

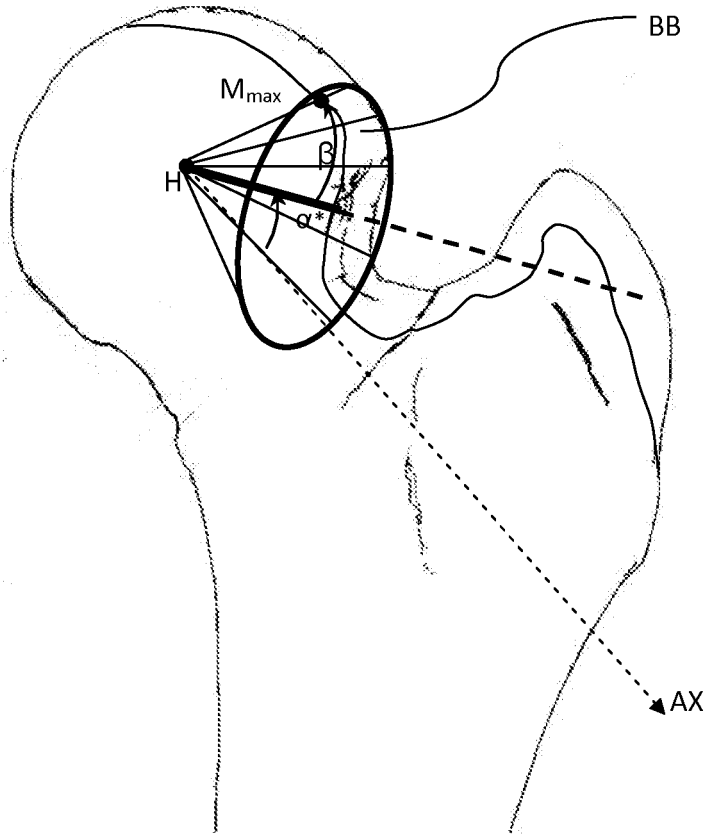

FIGURE 16B

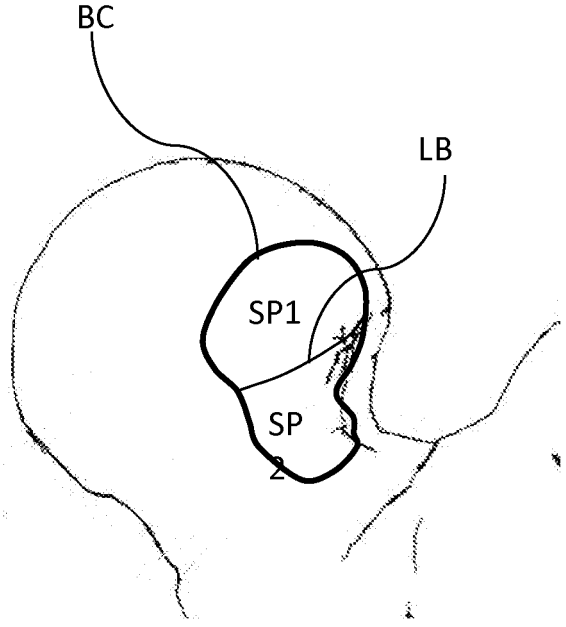

FIGURE17A

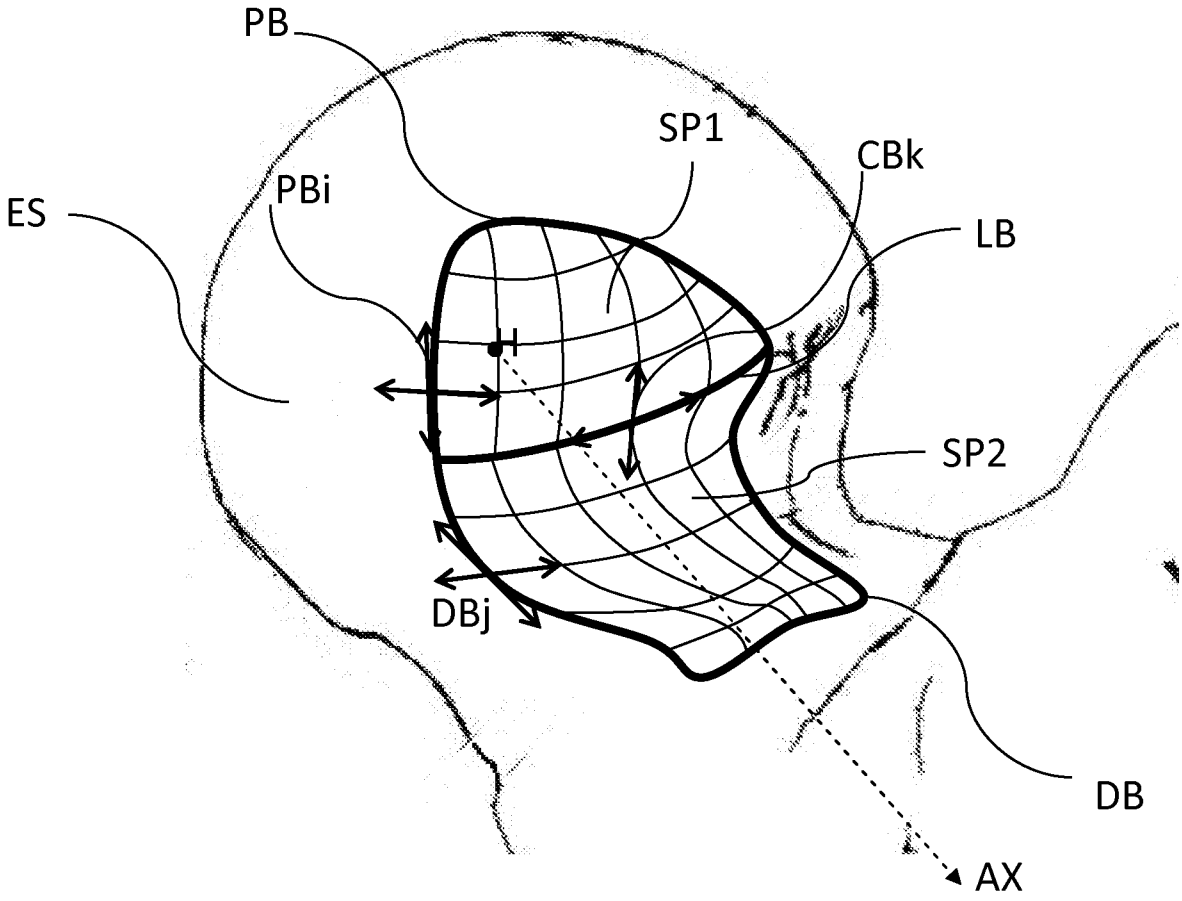

FIGURE 17B

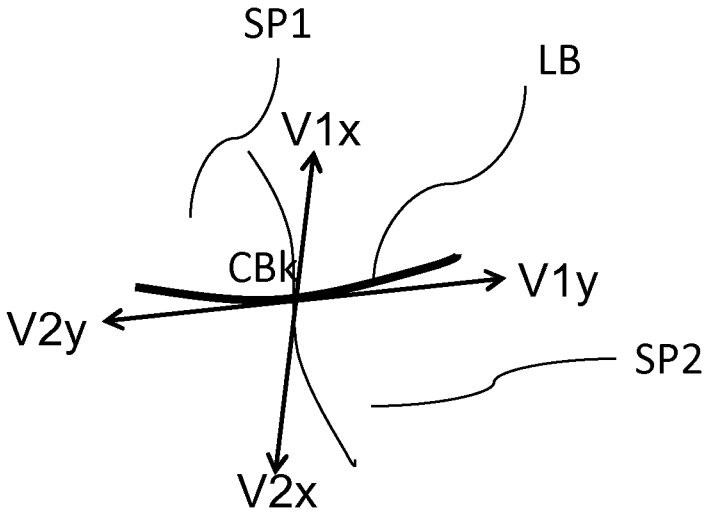

FIGURE 18A

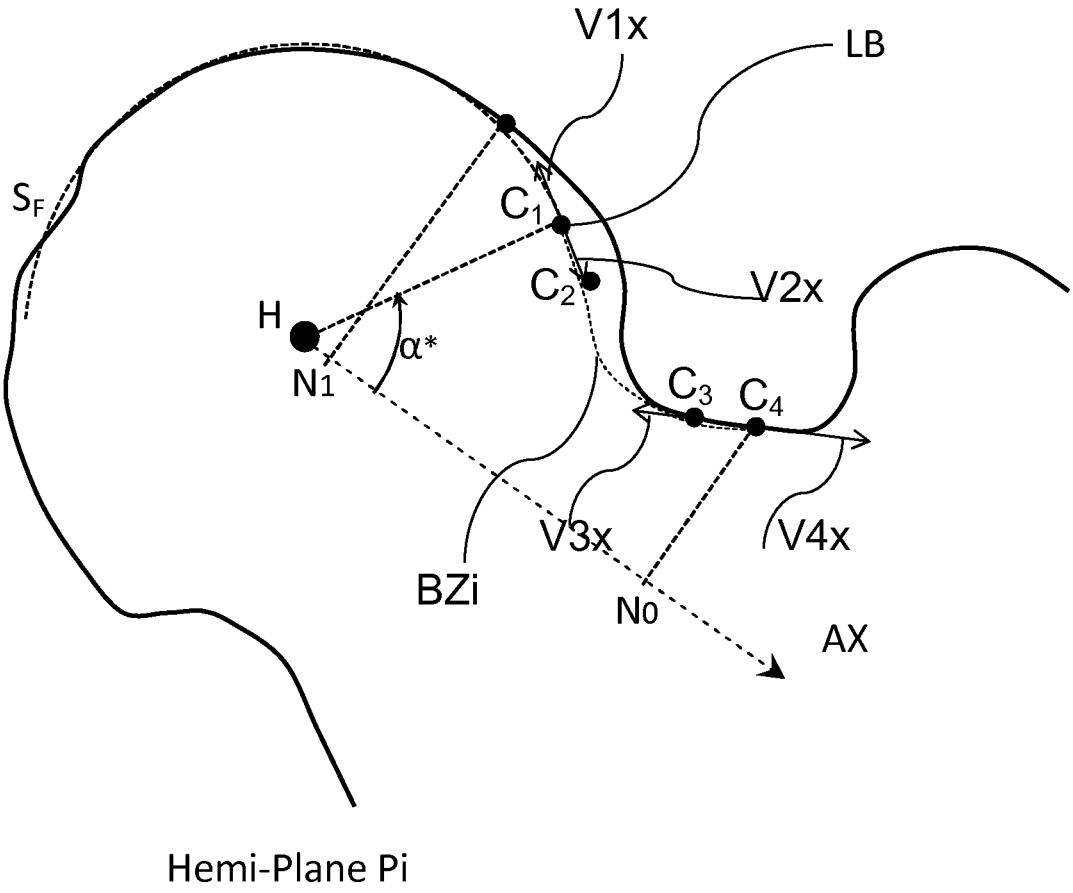

FIGURE 18B

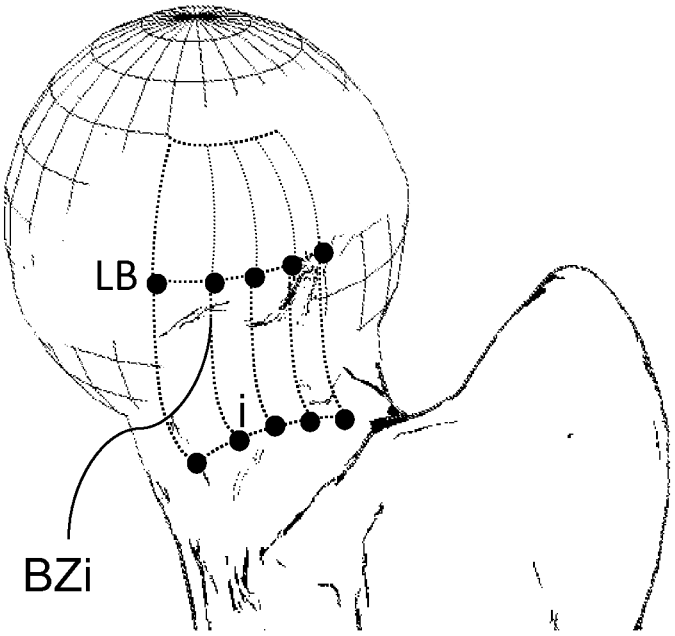

FIGURE 19A

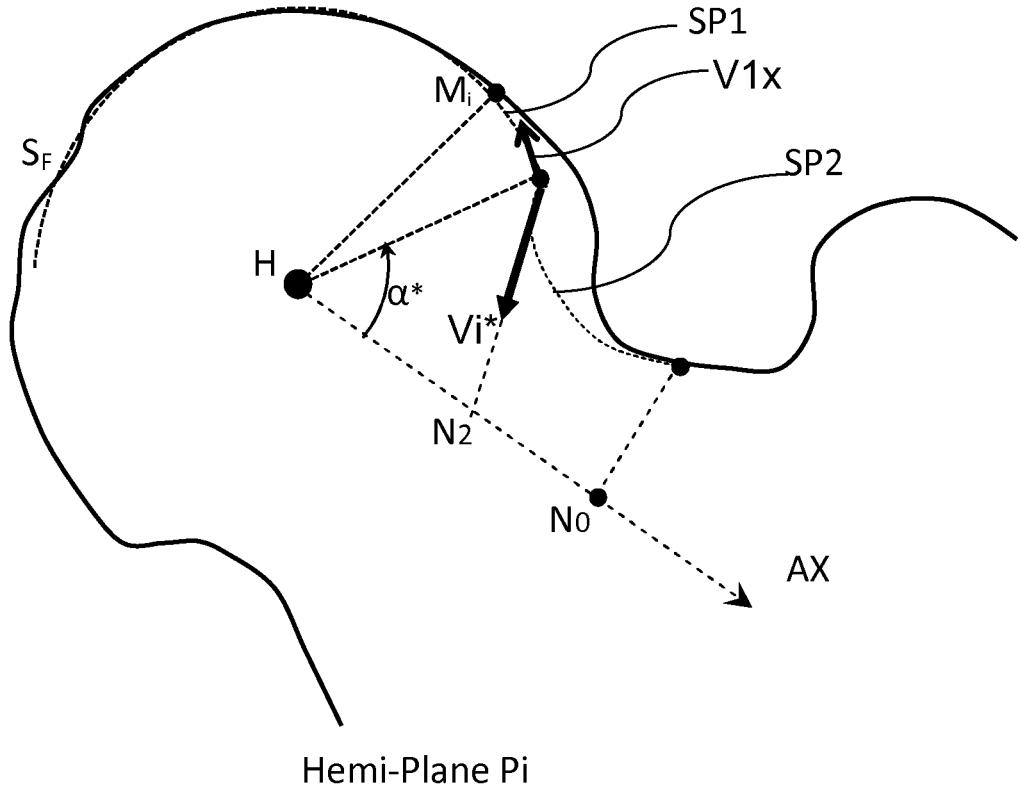

FIGURE 19B

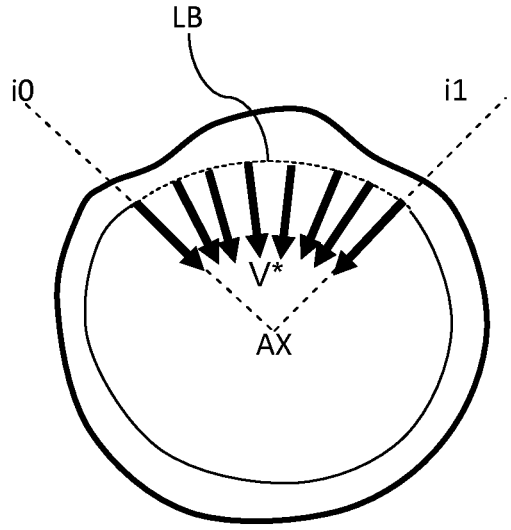

REFERENCES CITED IN THE DESCRIPTION

This list of references cited by the applicant is for the reader's convenience only. It does not form part of the European patent document. Even though great care has been taken in compiling the references, errors or omissions cannot be excluded and the EPO disclaims all liability in this regard.

Patent documents cited in the description

- US 20070249967 A1 **[0006]**

Non-patent literature cited in the description

- **NÖTZLI et al.** The contour of the femoral head-neck junction as a predictor for the risk of anterior impingement. *The Journal of Bone and Joint Surgery,* May 2002, vol. 84B (4 **[0006]**
- Computer-assisted pre-operative planning for hip joint-preserving surgery. **KANG et al.** Annual Meeting of the International Society for Computer Assisted Orthopaedic Surgery. Pro Business, June 2005, 212-214 **[0006]**
- Computer-assisted simulation of femoro-acetabular impingement surgery. **TANNAST et al.** Navigation and MIS in Orthopaedic Surgery. Springer, 2007, 440-447 **[0006]**

专利名称(译)	从几个参数确定变形骨表面上的骨切除的方法		
公开(公告)号	EP2583255B1	公开(公告)日	2019-07-24
申请号	EP2011764280	申请日	2011-06-16
[标]申请(专利权)人(译)	A2手术		
申请(专利权)人(译)	A²手术		
当前申请(专利权)人(译)	A²手术		
[标]发明人	CHABANAS LAURENCE LAVALLEE STEPHANE TONETTI JEROME BYRD THOMAS KELLY BRYAN TALMADGE LARSON CHRISTOPHER		
发明人	CHABANAS, LAURENCE LAVALLEE, STÉPHANE TONETTI, JÉRÔME BYRD, THOMAS KELLY, BRYAN TALMADGE LARSON, CHRISTOPHER		
IPC分类号	G06T19/20 G06T17/30 A61B5/00		
CPC分类号	G06T7/0012 G06T3/60 G06T5/002 G06T17/30 G06T19/20 G06T2210/41 G06T2219/2021		
优先权	61/355207 2010-06-16 US		
其他公开文献	EP2583255A2		
外部链接	Espacenet		

摘要(译)

本发明涉及一种用于非侵入性地可重复地确定3D骨表面模型上的校正表面的方法，所述3D骨表面模型由具有变形的骨的3D医学图像构成，所述变形包括头颈连接处的隆起过度生长;其中所述校正表面包括：i）在所述3D骨表面模型的头部上的3D球形校正表面贴片，以及ii）在所述3D骨表面模型的颈部上的3D平滑过渡校正表面贴片，其与所述3D邻接球面修正表面贴片;所述校正的表面斑块由一组参数限定，所述参数包括：iii）表示所述3D球形校正表面斑块的球形范围值的至少一个第一参数（a*），iv）和一组至少一个第二参数，所述设定确定所述经校正的表面斑块的3D校正边界，使得所述校正的表面斑块沿着所述边界与所述3D骨表面模型连续。

FIGURE 1